

c.1

**THE
PERIPHERAL JET PUMP: LABORATORY MODEL &
PRACTICAL APPLICATIONS FOR INCOMPRESSIBLE
MATERIALS TRANSPORT**

By

Paul Tamotsu Kadota

B.A.Sc. University of British Columbia, 1985

**A REPORT SUBMITTED IN PARTIAL FULFILLMENT OF
THE REQUIREMENTS FOR THE DEGREE OF
MASTER OF APPLIED SCIENCE**

in

**THE FACULTY OF GRADUATE STUDIES
DEPARTMENT OF CIVIL ENGINEERING
THE UNIVERSITY OF BRITISH COLUMBIA**

**We accept this report as conforming
to the required standard**

THE UNIVERSITY OF BRITISH COLUMBIA

March 1988

©Paul Tamotsu Kadota, 1988

In presenting this thesis in partial fulfilment of the requirements for an advanced degree at the University of British Columbia, I agree that the Library shall make it freely available for reference and study. I further agree that permission for extensive copying of this thesis for scholarly purposes may be granted by the head of my department or by his or her representatives. It is understood that copying or publication of this thesis for financial gain shall not be allowed without my written permission.

Department of CIVIL ENGINEERING

The University of British Columbia
1956 Main Mall
Vancouver, Canada
V6T 1Y3

Date APRIL 28, 1988

Abstract

The peripheral jet pump is examined in both theoretical and in practical applications. One-dimensional, force-momentum theory is applied in a jet pump setting for incompressible fluids. Results from a laboratory model are used for applications design. The scope of practical applications examined include:

- 1) use as a fish pump,
- 2) as part of a crab-sampling device,
- 3) feasibility as a ship's bow thruster.

The laboratory tests revealed the inadequacy of the current theory for wide jet spray patterns. The benefit of wide jets on suction and non-benefit on lift performance were established. Other performance aiding factors such partial submergence, partial blockage, and having the jets located at the suction inlet are studied for one phase, two phase and three phase pumping.

Also, as a complement to the written theory, computer programs which model the theoretical performance of peripheral jet pumps are available on 5.25" floppy disks. The programs are written for use on IBM PC and compatible computers.¹

¹IBM is a registered trademark of International Business Machines.

TABLE OF CONTENTS

<i>Abstract</i>	ii
<i>List of Figures</i>	iv
<i>Acknowledgements</i>	vi
<i>Nomenclature</i>	vii
1. INTRODUCTION.....	1
2. BASIC THEORY.....	6
3. LABORATORY TESTING.....	14
3.1 Purpose.....	15
3.2 The Test Circuit.....	16
3.3 Testing The One-Dimensional Theory.....	20
3.4 Testing Differences in Jet Configuration.....	23
3.5 Testing For Solids-Handling Capability.....	31
4. APPLICATIONS IN FISH TRANSPORT.....	36
4.1 System Analysis.....	37
4.2 Experimental Procedures.....	41
4.3 Results.....	45
5. APPLICATIONS IN A CRAB SAMPLING DEVICE.....	50
5.1 System Analysis.....	51
5.2 Experiments & Results.....	52
6. APPLICATION AS A BOW THRUSTER.....	56
6.1 System Analysis.....	58
7. DISCUSSION.....	61
8. CONCLUSIONS.....	66
9. REFERENCES.....	68

List of Figures

Fig. 1: A Typical Peripheral Jet Pump.....	2
Fig. 2: A Typical Single-Jet Ejector.....	2
Fig. 3: Control Volume for the Peripheral Jet Pump.....	8
Fig. 4: The Laboratory Model.....	14
Fig. 5: Laboratory Set-up.....	16
Fig. 6: Jet Rings for the Laboratory Model.....	19
Fig. 7: Comparing Experiment with Theory.....	20
Fig. 8: Drilled vs. Effective Jet Angles.....	22
Fig. 9: System Head Curves.....	24
Fig. 10: Vacuum Test Apparatus.....	25
Fig. 11: Variation of Vacuum vs. %Closure.....	26
Fig. 12: Air Gaps Between the Jets.....	27
Fig. 13: Variation of Vacuum vs. Applied Pressure.....	28
Fig. 14: Point of Solids Injection.....	31
Fig. 15: Partial Submergence.....	34
Fig. 16: A Prototype Fish Pumping System.....	36
Fig. 17: System Analysis.....	38
Fig. 18: System Head Test.....	41
Fig. 19: Suction Head Test.....	42
Fig. 20: Static Lift Test.....	43
Fig. 21: Dynamic Lift Test.....	44
Fig. 22: System Heads.....	45
Fig. 23: Suction Heads.....	46
Fig. 24: Static Lifts.....	47
Fig. 25: Submerged, Unsubmerged & Partial Operation.....	48
Fig. 26: Prototype Crab Sampling Device.....	50

Fig. 27: Sampling Hood Details.....	53
Fig. 28: Minimizing Pick-up Time.....	54
Fig. 29: Propeller & Jet Thrusters.....	56
Fig. 30: Jet Pump Thruster.....	57
Fig. 31: Specific Thrust.....	59

Acknowledgements

I wish to thank Dr. Michael Quick of the University of British Columbia for being my mentor and for his counsel in many aspects of this project. Also, I would like to acknowledge the support of all the technicians in the Department of Civil Engineering for their wisdom in the manufacture of the jet pump prototypes.

Special thanks to Mr. Michael Shields of Shields Navigation Limited and Mr. Alan Westfall, for their experience and knowledge of peripheral jet pumps. I would also like to thank the Department of Fisheries and Oceans for their support in the development of the crab sampling device.

This project was made possible by grants from both Shields Navigation Limited, and the National Research Council's Industrial Research Assistance Program (IRAP-H).

Nomenclature

A	total suction area of jet pump inlet
A_j	total area of jets
g	gravitational acceleration
h_1	head loss due to jet pump shear components
h_2	head loss due to manifold and jet losses
H_d	total head at discharge
H_j	total head at jet exit
H_m	total head at manifold, prior to entrance
H_s	total head at suction
K_1	friction factor associated with T_i
K_2	friction factor associated with manifold and jet losses
M	defined as the flow ratio = Q_s/Q_m
N	defined as the head ratio = $(H_d - H_s)/(H_m - H_s)$
P_d	assumed even pressure at discharge
P_j	assumed even pressure at jet exit, assumed = P_s
P_m	hydraulic pressure applied to jet pump manifold
P_s	assumed even pressure at suction, assumed = P_j
Q_d	discharge flow of the jet pump = $Q_s + Q_m$
Q_j	jet flow from the manifold flow, $Q_m = Q_j$
Q_m	manifold flow which supplies the jet flow, $Q_j = Q_m$
Q_s	suction flow of the jet pump at intake
R	defined as the area ratio of A_j/A
$R.L.$	relative jet-hole length = (jet length)/(diameter)
T_i	jet pump shear components assumed to be a function of Q_d only
V_d	velocity of discharge flow
V_j	average velocity of jet flow = Q_m/A_j
V_s	velocity of suction flow
n	efficiency of jet pump = NM
Θ	jet angle with respect to pump axis
ρ	fluid density

1. INTRODUCTION

The peripheral jet pump is often regarded as the pump with no moving parts. In place of impellers or propellers used in conventional centrifugal and axial pumps, it uses water jets instead. In addition to its ease of installation, the jet pump's other advantages are, simplicity, reliability, and its ability to pump gases, liquids and solids simultaneously. Its major disadvantage is its inferior efficiency. While centrifugal pumps have maximum efficiencies upwards of 80%, the jet pump on the other hand, have maximums generally half this value.

The operating principle of jet pumps is the transfer of momentum by a high-pressure stream of fluid into an existing body of fluid. The high-pressure jets create a low-pressure area in the mixing chamber, causing suction fluid to be fed into the high-velocity area of the jets (see figure 1). At this point, the suction fluid exchanges momentum with the jets. Ideally, there is complete mixing of the suction fluid and the jets, such that the mixed stream travels at an uniform velocity.

In reality, the mixed stream is never thoroughly mixed, and an uniform velocity is not achieved. However, if the average velocity of the mixed stream could be calculated, it would lie somewhere between the velocities of the jet and suction fluids. Complete mixing in the control volume is one of the assumptions made in the theoretical analysis.

The basic theory is reasonably well understood when a single phase, such as water, is considered. The theory has not been extended for two or three phase operation, when, for example, a mixture of air and water or a mixture of air, water and solids is being drawn into the pump. One aim of this work is to investigate the influence of air and solids on the performance of the jet pump. Various designs of jet arrangements will be tested to determine possible benefits or non-benefits.

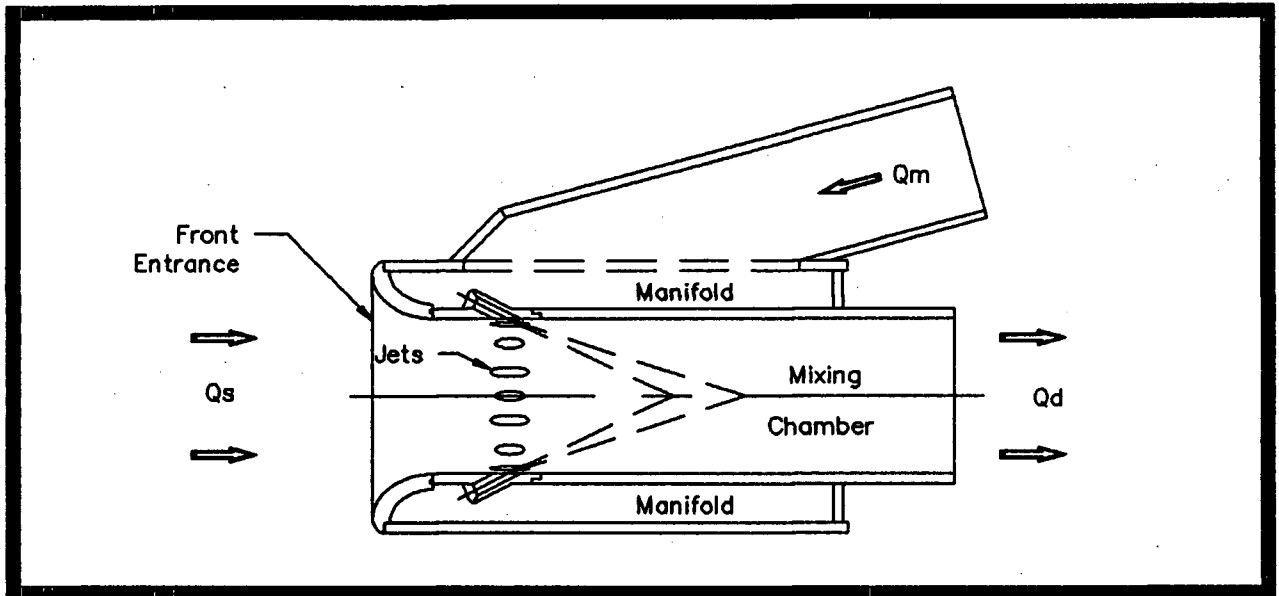


Fig. 1: A Typical Peripheral Jet Pump

Besides the peripheral jet pump, the more common single-jet ejector is shown in figure 2. They are usually housed in a venturi-like geometry to help increase the velocity of the suction flow. The contraction causes the suction fluid to accelerate towards the throat, where it attains maximum velocity. Then the fluid decelerates as the mixed flow expands in the diffusing section.

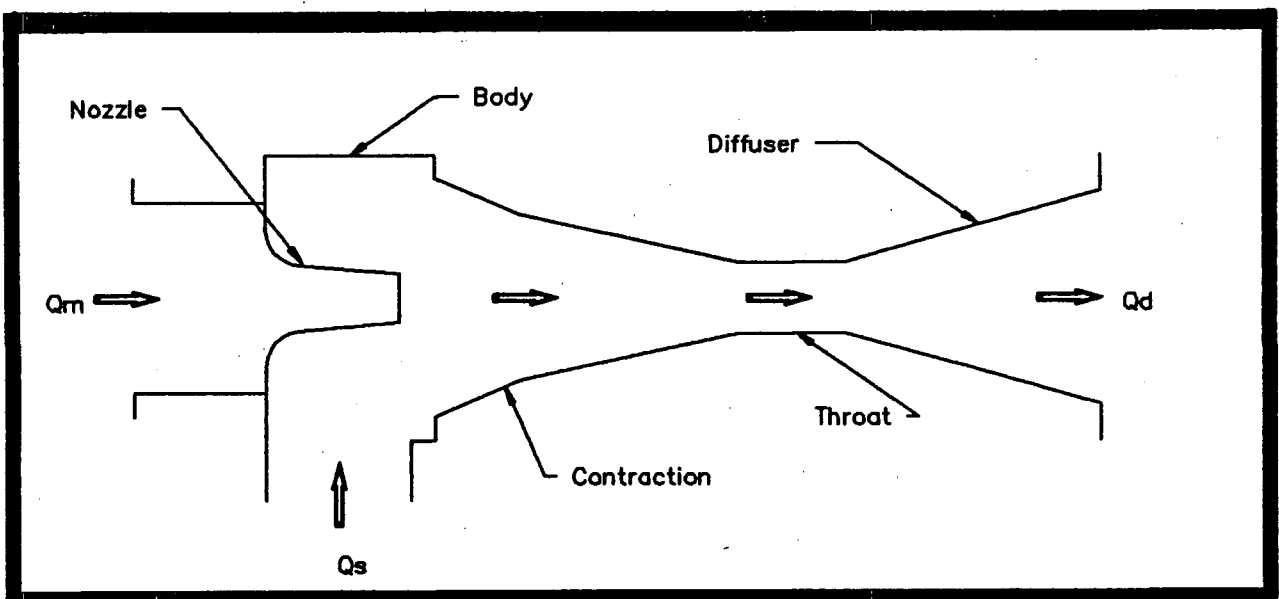


Fig. 2: A Typical Single-Jet Ejector

Although the single-jet ejector is more common than the peripheral ejector, it physically limits the maximum size of solids in the suction fluid. But for the peripheral jet pump in figure 1, since the suction fluid is not subject to contraction and expansion changes, clogging will not be a problem. Therefore, the peripheral jet pump is the practical choice for moving suction fluids with large solids contents.

With the added benefits of having no moving parts and being self-priming, the jet pump has a broad range of applications. This paper will focus on applications in fish and juvenile crab handling and as a ship's bow thruster. These are not common applications for a jet pump, but it exemplifies the versatility of the jet pump concept. As a matter of interest, some of the more common applications of jet pumps are given below:

Mixing eductors, used for proportioning liquids in chemical processing industries.

Slurry eductors, for pumping out wells, pits, tanks, sumps and similar reservoirs where sand, mud or slime accumulate. Absence of impellers make the jet pump an ideal candidate for this application.

Deep-Well eductors, assist conventional mechanical pumps to draw water up from a deep well. Jet pumps are located at the base of the well, and the mechanical pump at the top. The jet pump's discharge is connected in series with the suction of the mechanical pump. This boosts the suction pressure of the mechanical pump, thus preventing cavitation problems.

Solids-handling eductors, located at the base of a hopper for moving granular solids. The jet nozzle shoots into a mixing chamber, which constitutes the beginning of the transportation lines. Construction of the jet nozzle is typically reinforced with hardened steel, preventing premature wear.

Suggested Reading

Chapter 2 deals with the theoretical foundation for the peripheral jet pump. Several assumptions were made to simplify the theory as much as possible. As such, the formulation presented here is one of the simplest theories for modelling jet pump performance. This chapter may be omitted if the reader is primarily interested in the applications.

Chapter 3 describes experiments on a laboratory jet pump model. Tests were conducted to compare results against theory, and to determine the effects of changes in the jet configuration. New views on analyzing the data were established. Many of the tests conducted are not documented anywhere else in current literature.

Chapter 4 describes a complete prototype of a fish-pumping system. Some of the knowledge gained from tests on the laboratory model were incorporated. Experimental tests and results of four basic tests are given:

- 1) The System Head tests verify the basic theory of jet pump characteristics. These results are required for the selection of the proper mechanical pump.
- 2) The Suction Head tests, measures the potential suction capabilities of the jet pump.
- 3) The Static Lift tests verify the lifting potential of the jet pump and it measures the pump's ability to hold a static column of water.
- 4) The Qualitative Dynamic Lift tests were done primarily to observe the jet pump in normal fish-pumping operation.

Chapter 5 explains how the jet pump was used as part of a juvenile-crab sampling system. The Department of Fisheries and Oceans, required a portable device which brought samples of crabs from the bottom of the sea to the water surface. Crabs measuring up to 50mm (2") across its back were used as test specimens.

Chapter 6 briefly examines the feasibility of using the peripheral jet pump as a ship's bow thruster. A prototype of a bow thruster was not made.

2. BASIC THEORY

Three Approaches

Recent investigation of the jet pump literature reveals at least three approaches for the prediction of jet pump performance:

- 1) **One-dimensional analysis** is used to simplify a three dimensional problem to a single dimension and uses momentum and energy laws to solve for pressure and flow ratios. This is the simplest and most often used method. See papers by, Cunningham (3), Henzler (4), Jumpeter (8), Kentfield et al (9) and Westfall (13).
- 2) **Two-dimensional analysis** reduces a three dimensional problem to a two-dimensional one. By means of Prandtl and Taylor's theory, elliptic partial differential equations for the time-averaged velocity in the x & y directions are solved. Using the Poisson equation for pressure correction, a first approximation to the solution is found. This is followed by a succeeding correction then a second approximation. This iterative procedure continues until the corrections become sufficiently small. See papers by, Charlesworth et al (2), Hill (6) and Hongji et al (7).
- 3) **Approximation theory and statistical methods**; In his paper, Xianghan (15) outlines a method of using experimental data to derive empirical formulas to predict jet pump performance. From his experimental results, he begins by defining the performance equations as a function of all affecting parameters. Then he approximates the functions with a group of polynomials, which he subsequently substitutes with equivalent linear factors. Expansion into standard linear equations follows, which are then solved using multivariate step-by-step regression and orthogonal polynomial methods.

Xianghan's exhaustive test results show that, the one or two-dimensional theory

cannot correctly describe the jet pump's performance. Both the one and two dimensional theories claim that non-dimensional performance curves for pumps which are geometrically similar, but having different absolute size, are identical. However, Xianghan has found this to be untrue. He says that although the general shape of the non-dimensional performance curve can be predicted, the actual curve cannot be reliably predicted unless each pump is tested, and its assumed loss factors recalculated. Therefore, Xianghan advocates the approximation and statistical method.

The one-dimensional analysis was used as the theoretical foundation for this paper. It was chosen because of its simplicity and its general acceptance in the jet pump community. Furthermore, use of one of the other two methods would have hindered reaching the goal of this thesis.

One-Dimensional Analysis

The basic peripheral jet pump theory outlined here is similar to that of Westfall's in his thesis paper.¹ The theory covers only the intrinsic characteristics of the peripheral jet pump. It does not consider any other component of the jet pump system. Therefore, the final function given by equation [2.18] can be considered to be the pump curve. The chapters on practical applications will analyze the system curve, so that the intersection of the two curves will predict the operating point.

¹Westfall, Alan Patrick, "Peripheral Jet Pump Theory and Experiment" (14).8

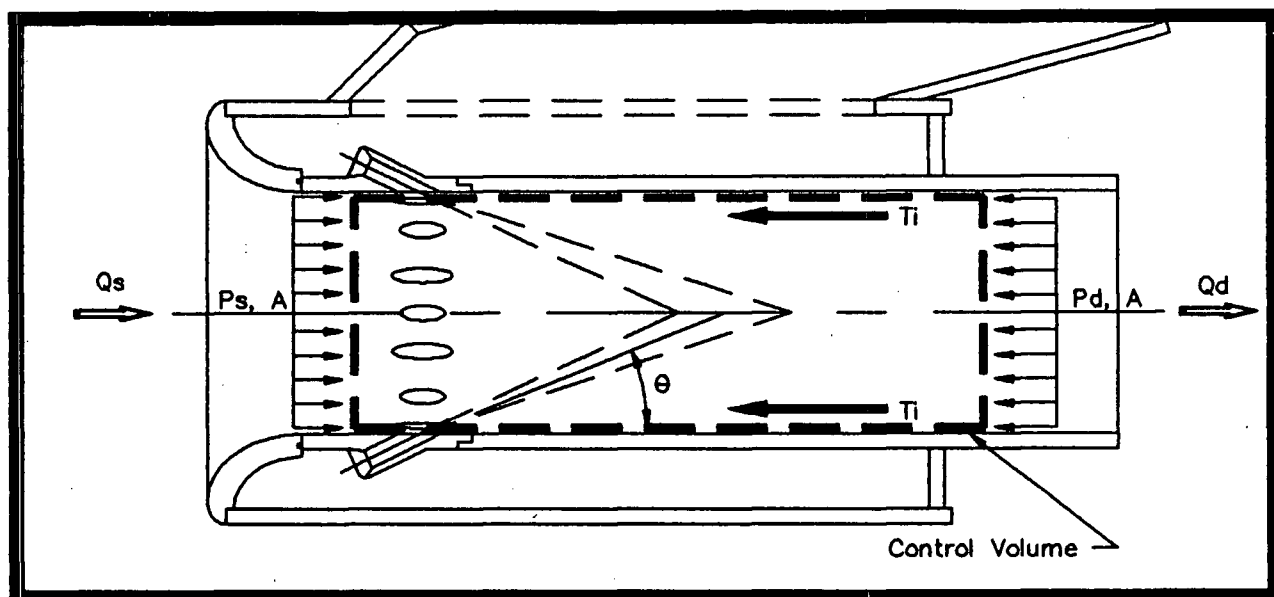


Fig. 3: Control Volume for the Peripheral Jet Pump

Analysis of the pumping action of the jet pump is rather complex if simplifications are not made. The complexity of the flow patterns within the mixing chamber makes it necessary to make some assumptions. For this analysis, a cylindrical control volume given in figure 3, will be assumed. Other assumptions include:

- 1) One-dimensional flow of incompressible fluids.
- 2) Complete mixing of the flow within the control volume.
- 3) Fluid densities are constant throughout.
- 4) No secondary or recirculating flows.
- 5) Cavitation does not occur.
- 6) Jet and manifold losses can be represented as a function of the jet velocity.
- 7) Wall friction losses can be represented as a function of the average discharge velocity.

Continuity, Energy (Bernoulli), and Momentum principles will be used in deriving the final pump equation [2.18].

Defining Non-Dimensional Parameters

Following conventions established for jet pumps, non-dimensional parameters M , N & R will be defined. M is the flow ratio of the suction fluid over the driving fluid. N is the head ratio between the discharge and the driving fluid, with respect to the suction head. R is the area ratio between the jet area and the suction area.

$$M = \frac{Q_s}{Q_m} \quad [2.1]$$

$$N = \frac{H_d - H_s}{H_m - H_s} \quad [2.2]$$

$$R = \frac{A_j}{A} \quad [2.3]$$

Defining Efficiency

Efficiency is normally defined as the ratio or percentage of the useful power output over the power input. For the case of jet pumps, the useful power output must be defined carefully so that you will not over exaggerate the value of the pump's efficiency.

Fluid power can be calculated given both the flow and the head of the fluid.

Flow: The total output flow is $Q_s + Q_m$, however, Q_m , the flow contributed from the driving fluid is generally regarded as a useless by-product of the momentum transfer. A good analogy would be heat energy given off by an engine. The heat is considered as a useless by-product of the combustion reaction, and is not considered in efficiency calculations. Therefore, only Q_s , the suction fluid, is used in jet pump efficiency calculations.

Head: Here, the determination of usefulness is straightforward. The entire head created by the momentum transfer is considered useful.² Therefore, the discharge head, H_d is used for calculations. But since this analysis strives for the intrinsic solution, both the output head, H_d , and the input head, H_m , are referenced with respect to the suction-side of the jet pump. In other words, the datum for energy heads is, H_s . Thus, for efficiency concerns, the output head and the input head are: $(H_d - H_s)$ and $(H_m - H_s)$ respectively.

Thus, the efficiency relationship is defined as follows:

$$n = \frac{\text{power output}}{\text{power input}} = \frac{Q_s \rho g (H_d - H_s)}{Q_m \rho g (H_m - H_s)} \quad [2.4]$$

In non-dimensional form:

$$n = MN \quad [2.5]$$

Continuity

Assuming the drive fluid and the pumped fluid have the same properties and the flow is incompressible,

$$Q_s + Q_m = Q_d$$

Using [2.3], this can also be written as:

$$\begin{aligned} V_s A + V_j A R &= V_d A \\ V_s + V_j R &= V_d \end{aligned} \quad [2.6]$$

²This holds true since we are assuming complete mixing.

Force-Momentum Relationship

Refer to Figure 3, for the assumed control volume. A force balance in the x-direction on this cylindrical mixing chamber gives:

$$P_s A - P_d A - T_i = p Q_d V_d - p Q_s V_s - p Q_j V_j \cos \Theta \quad [2.7]$$

Where T_i = wall friction shear force in the x-direction. It can be represented by a head-loss coefficient, K_1 , referred to the discharge velocity, V_d .

$$T_i = A p g K_1 \frac{V_d^2}{2g} \quad [2.8]$$

Putting flows in terms of velocities, equation [2.7] becomes:

$$A(P_s - P_d) - T_i = p V_d^2 A - p V_s^2 A - p V_j^2 A_j \cos \Theta$$

Using [2.3] to replace A_j , and after some rearranging of terms:

$$-T_i = p A (V_d^2 - V_s^2 - V_j^2 R \cos \Theta) + A (P_s - P_d) \quad [2.9]$$

Bernoulli Theorem (Energy)

Apply the Bernoulli theorem at suction, discharge, and between manifold and jet exits, and assume datum, $Z_s = Z_d = Z_m = Z_j = 0$.

$$H_s = \frac{P_s}{\rho g} + \frac{V_s^2}{2g} + Z_s \quad [2.10]$$

$$H_d = \frac{P_d}{\rho g} + \frac{V_d^2}{2g} + Z_d \quad [2.11]$$

$$H_m = H_j + K_2 \frac{V_j^2}{2g} \quad [2.12]$$

Apply equations [2.10] & [2.11] to equation [2.9].

$$-T_i = p A (V_d^2 - V_s^2 - V_j^2 R \cos \Theta) + A p g \left[\left(H_d - \frac{V_d^2}{2g} \right) - \left(H_s - \frac{V_s^2}{2g} \right) \right]$$

$$-T_i = p A (V_d^2/2 - V_s^2/2 - V_j^2 R \cos \Theta) + A p g (H_d - H_s)$$

Now use [2.8] and rearrange, solving for $H_d - H_s$.

$$H_d - H_s = \frac{2V_j^2 R \cos \Theta - (K_1 + 1)V_d^2 + V_s^2}{2g} \quad [2.13]$$

Also, from continuity and flow ratio [2.1], the following can be derived:

$$\begin{aligned} Q_s &= MQ_m = MQ_j \\ V_s A &= V_j AMR \\ V_s &= V_j MR \end{aligned} \quad [2.14]$$

Substitute [2.6] for V_s , and solve for V_d .

$$V_d = V_j R (M + 1) \quad [2.15]$$

Substitute [2.14] & [2.15] into [2.13].

$$H_d - H_s = \frac{V_j^2}{2g} (2R \cos \Theta - (K_1 + 1)(R(M + 1))^2 + (RM)^2) \quad [2.16]$$

Now, obtain expression for $H_m - H_s$, using [2.10] & [2.12].

$$H_m - H_s = H_j + \frac{K_2 V_j^2}{2g} - \frac{P_s}{pg} - \frac{V_s^2}{2g}$$

Replace H_j with pressure and velocity equivalents, noting that $P_j = P_s$.

$$H_m - H_s = \frac{P_j}{pg} + \frac{V_j^2}{2g} + \frac{K_2 V_j^2}{2g} - \frac{P_s}{pg} - \frac{V_s^2}{2g}$$

Now substitute for V_s using [2.14].

$$H_m - H_s = \frac{V_j^2}{2g} (1 + K_2 - (RM)^2) \quad [2.17]$$

Final Non-Dimensional Head Difference Ratio

Back in equation [2.2], N was defined as the ratio of the discharge head and the manifold head, both referenced with respect to the suction head. As can be seen, equation [2.16] forms the numerator of that ratio, and equation [2.17] forms the denominator. Thus, by combining these two equations, N will be expressed in terms of non-dimensional parameters.

$$N = \frac{H_d - H_s}{H_m - H_s} = \frac{(2R\cos\Theta - (K_1 + 1)(R(M + 1))^2 + (RM)^2)}{(1 + K_2 - (RM)^2)} \quad [2.18]$$

The pressure ratio, N , can thus be solved given the constants, Θ , K_1 and K_2 , and the dimensionless parameters, R & M .

3. LABORATORY TESTING

The 2.5" Laboratory Model

Prior to manufacturing full-size prototypes, a small 63mm (2.5") diameter jet pump model was made and tested at U.B.C.'s Civil Engineering Hydraulic Laboratory. Machined from aluminum and clear acrylic, this model was easy to disassemble, so that changes to the jets could be made within a matter of minutes. Figure 4 shows the structural workings of the model.

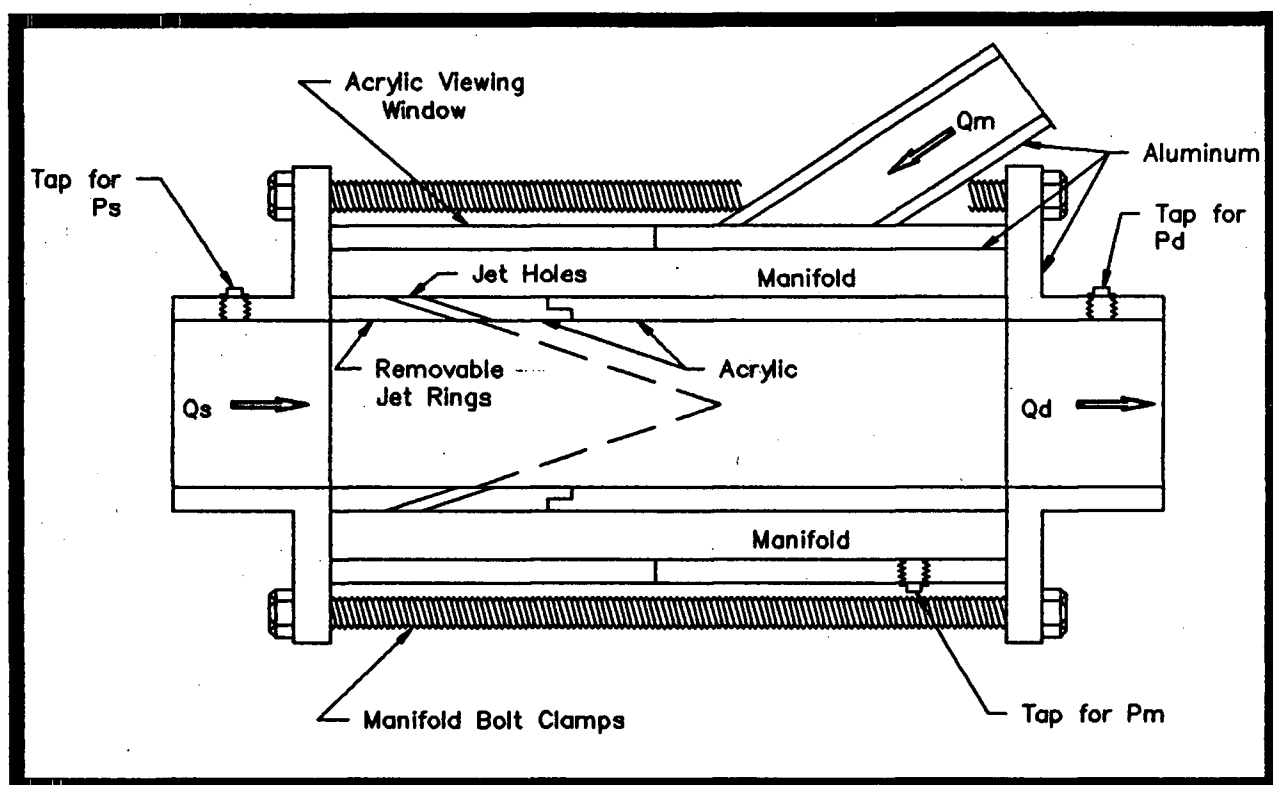


Fig. 4: The Laboratory Model

The aluminum provides the structural rigidity, while the clear acrylic provides visual windows into the jet pump's manifold, jet exits and the mixing chamber. A series of interchangeable jet "rings," each with different configurations were made and tested.

3.1 PURPOSE

The lab model served as the testing grounds for new design ideas. The effects of changing some of the structural parameters of the pump required investigation, so that an optimum design could be defined for each specific application. In particular, the goals for the model were:

- 1) Verify the one-dimensional jet pump theory.
- 2) Test the effects of changing the jet configuration, including: relative jet length, jet positions within the system and two rings of jets in series.
- 3) Study qualitatively the behaviour as a solids-handling pump in both a two-phase and three-phase setting. Two-phase meaning, liquids & gases or liquids & solids, and three-phase meaning, solids, liquids and gases. Then, define the optimum design of each.

3.2 THE TEST CIRCUIT

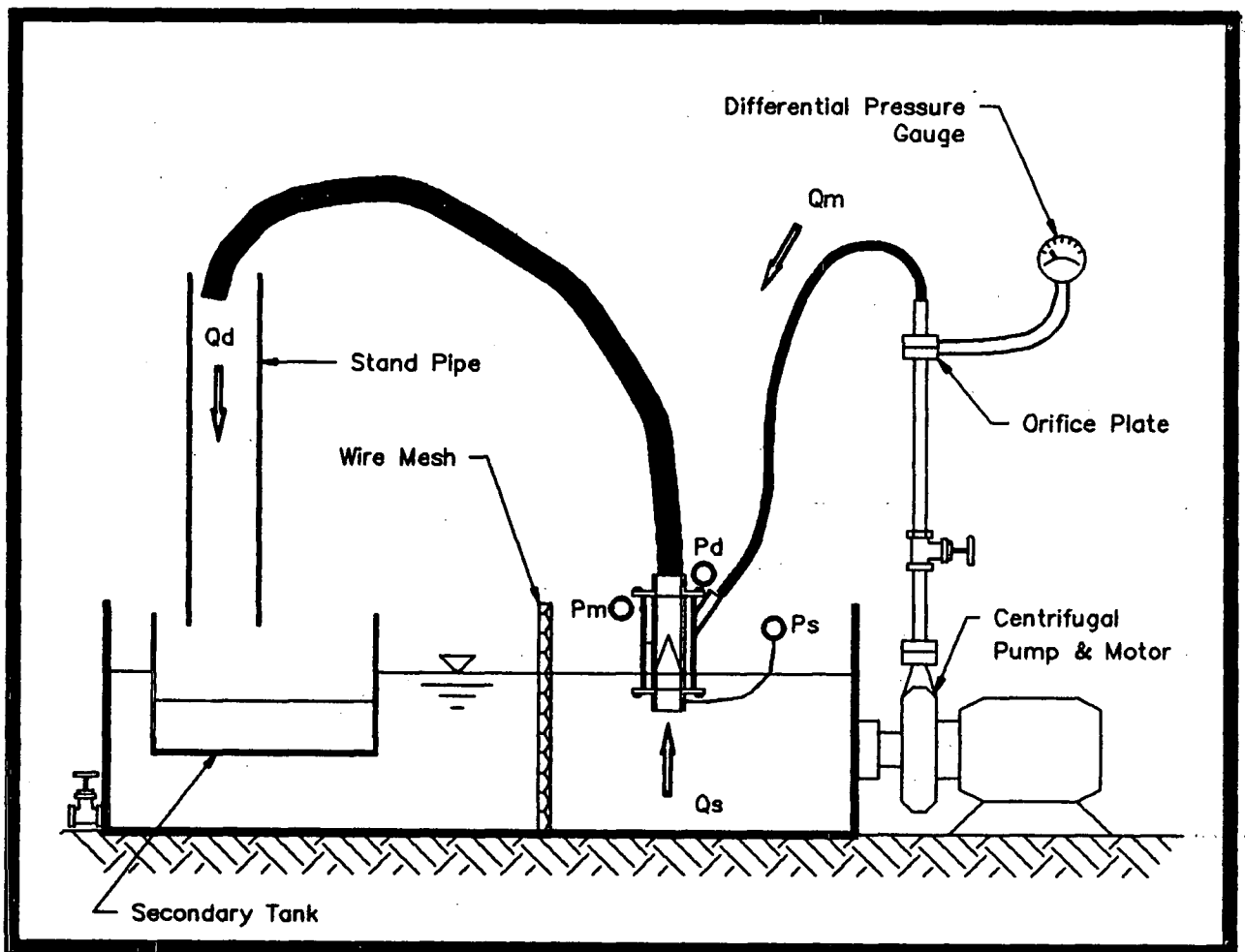


Fig. 5: Laboratory Set-up

The recirculating system consisted of a 1.5 x 1.8 x 0.76m (WxLxH) steel tank, a 38mm (1.5") centrifugal pump direct coupled to a 11.2kW (15HP) electric motor, PVC hoses and various pressure and flow measuring devices. Pressures were easily measured directly via gauges, however, flow measurements were done indirectly, either by an orifice plate, or volumetrically using a secondary tank.

Q_m , the manifold flow, was measured using the orifice plate and differential pressure gauge combination. This plate meter was precision machined and calibrated against volumetric measurements, prior to any jet pump testing. Q_d , the discharge flow, was measured volumetrically using a 0.9 x 1.1 x 0.5m (WxLxH) secondary tank. The secondary

tank was initially floated inside the larger primary tank, then filled with the discharge flow, Q_d . Floating the tank in this way kept the tank at constant level, while a discharge measurement was being made. This constant tank level maintains constant suction conditions, an important consideration when making measurements. The duration required to fill the secondary tank was timed. Dividing the tank volume by the duration gave the average discharge flow, Q_d .

The Jet Rings

Six jet ring configurations, each having the same area ratio, $R = 0.1225$, were tested. Other variables also held fixed were: jet angles @ 25° & 18° , total number of jets @ 16, and hole diameters @ 5.5mm (7/32"). The differences between the jet rings were in the jet-hole profiles, each with various combinations of jet-hole length and entrance shapes. The relative length of jets, R.L., is defined here as the quotient of the jet-hole length over the jet-hole diameter.

$$R.L. = \frac{(\text{Jet Length})}{(\text{Jet Diameter})} \quad [3.1]$$

In observation, the rings with the shortest R.L. gave the widest jet spray patterns. A summary of the different jet rings are given both in the table below and in figure 6.

Jet Ring Specifications

Ring Ref. #	No. of Jets	Dia. (mm)	Jet Angles (deg.)	Wall Thickness (mm)	Length of Jet (mm)	R.L.
1	16	5.5	25 & 18	12.7	38	6.9
2	16	5.5	25 & 18	6.4	19	3.4
2.1	16	5.5	25 & 18	6.4	13	2.4
3	16	5.5	25 & 18	19.1	48	8.7
3.1	16	5.5	25 & 18	19.1	14	2.5
Hillis	8+8	5.5	25 & 18	6.4	19	3.4

Rings #1 through #3.1 all have 16 jets drilled around a single perimeter location. Eight of these holes were drilled at a 25° degree angle and eight were drilled at a 18° angle.

The Hillis ring, however, was drilled at two separate perimeter locations. A total of 16 holes were drilled, with 8 holes at each of the two locations. Again, the angles were held constant at 25° for the first and 18° for the second perimeter location.

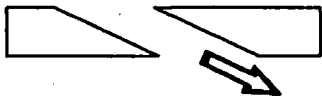
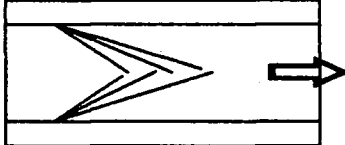
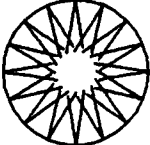
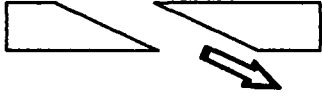
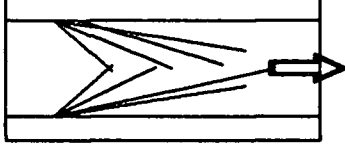
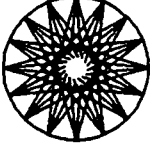
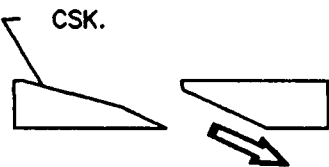
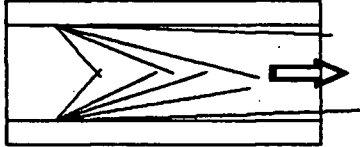
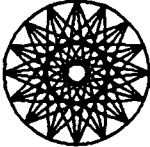
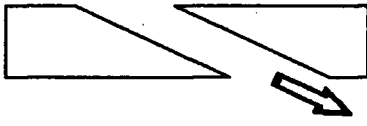
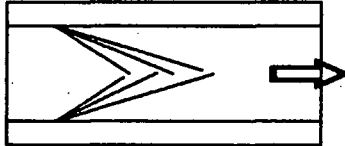
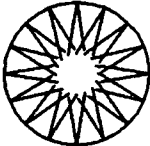
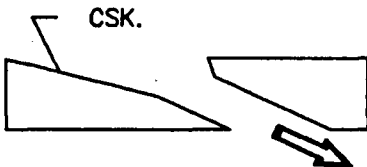
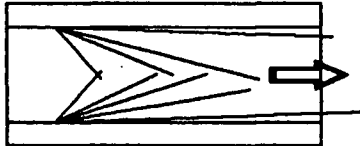
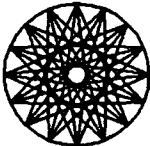
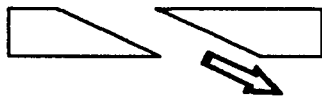
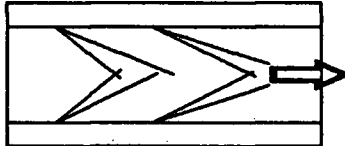
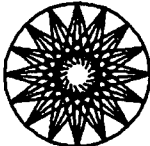
#	Jet Hole Profile	Side View of Spray Pattern	Axial View of Spray Pattern
1			
2			
2.1			
3			
3.1			
Hillis			

Fig. 6: Jet Rings for the Laboratory Model

3.3 TESTING THE ONE-DIMENSIONAL THEORY

Testing the one-dimensional theory according to equation [2.18] was done with apparatus similar to that of figure 5. The suction-side of the jet nozzle was submerged 4" below the water surface. This was found to be sufficient depth to prevent air-entraining vortex formation. All recorded measurements were done with the jet pump in a steady-state, single-liquid phase. Any trapped air in the hoses were pumped out prior to taking any measurements. The manifold pressure, P_m , was varied for pressures up to 415kPa (60psi). This procedure was repeated for all six jet rings, then the results were plotted in non-dimensional form.

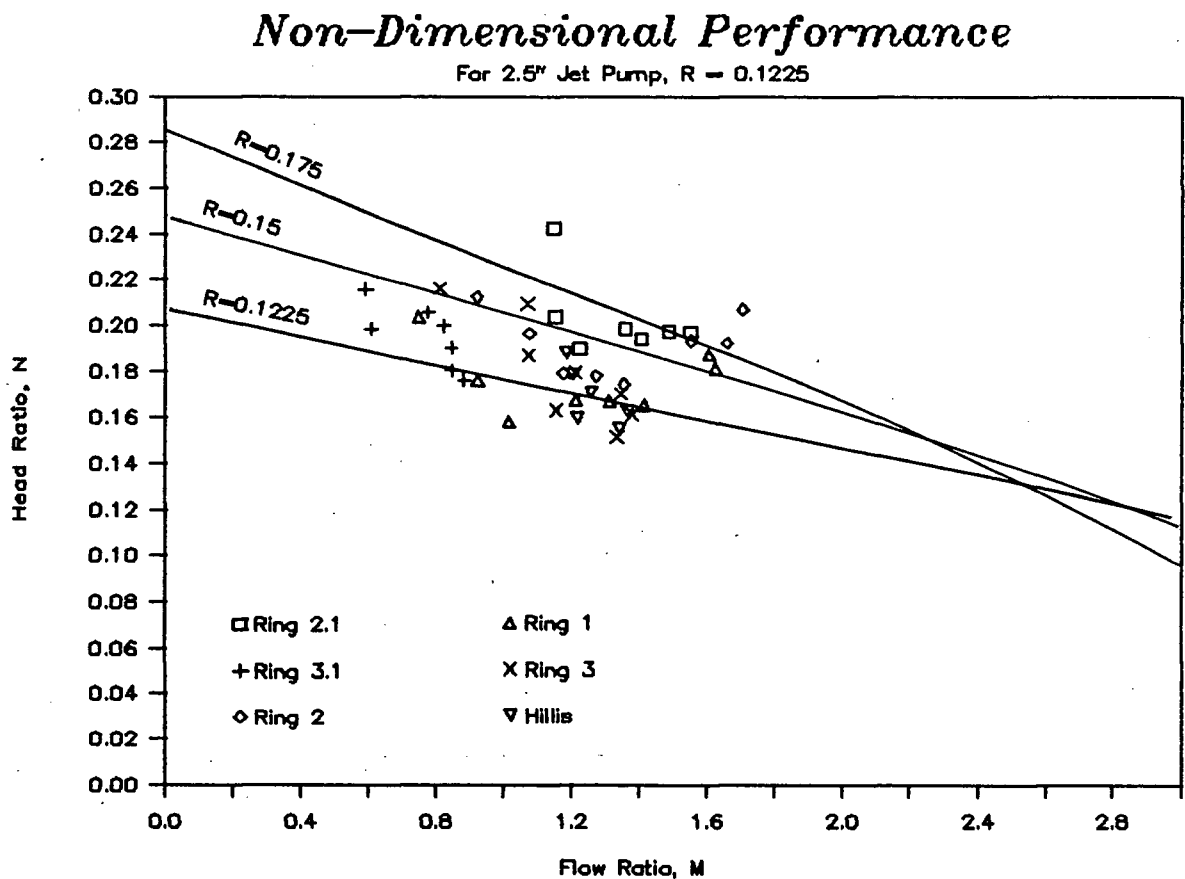


Fig. 7: Comparing Experiment with Theory

Results

Figure 7 shows a N vs. M non-dimensional performance curve of the six jet rings. As can be seen, adherence to the one-dimensional theory for $R = 0.1225$, is not good for all the jet rings. The data points lie generally above the $R = 0.1225$ line, closer to the $R = 0.15$ line.

In particular, for ring #2.1, the points are scattered closer to the $R = 0.175$ line. One explanation for this deviation is that ring #2.1 has a larger effective area ratio, R . Referring to figure 6, the jet hole profile for ring #2.1 is counter-sunk. Therefore, although the holes were originally drilled at 5.5mm, counter-sinking of the jet profile changed the flow pattern, effectively enlarging the diameter to 6.6mm.

Another reason for the experimental deviations is the break-down of the jet spray patterns. Long relative jet lengths produced solid narrow jet spray, while short relative jet lengths produced a wide jet spray. Figure 8 illustrates this point. For the narrow jet spray, maintaining the drilled jet angle is easy. Therefore, it correlates better to the one-dimensional theory. But for the wide jet spray, maintaining the assumed drilled jet angle may be difficult. The effective jet angle, and drilled jet angle will in fact be different, and this will cause discrepancies between theory and experiment.

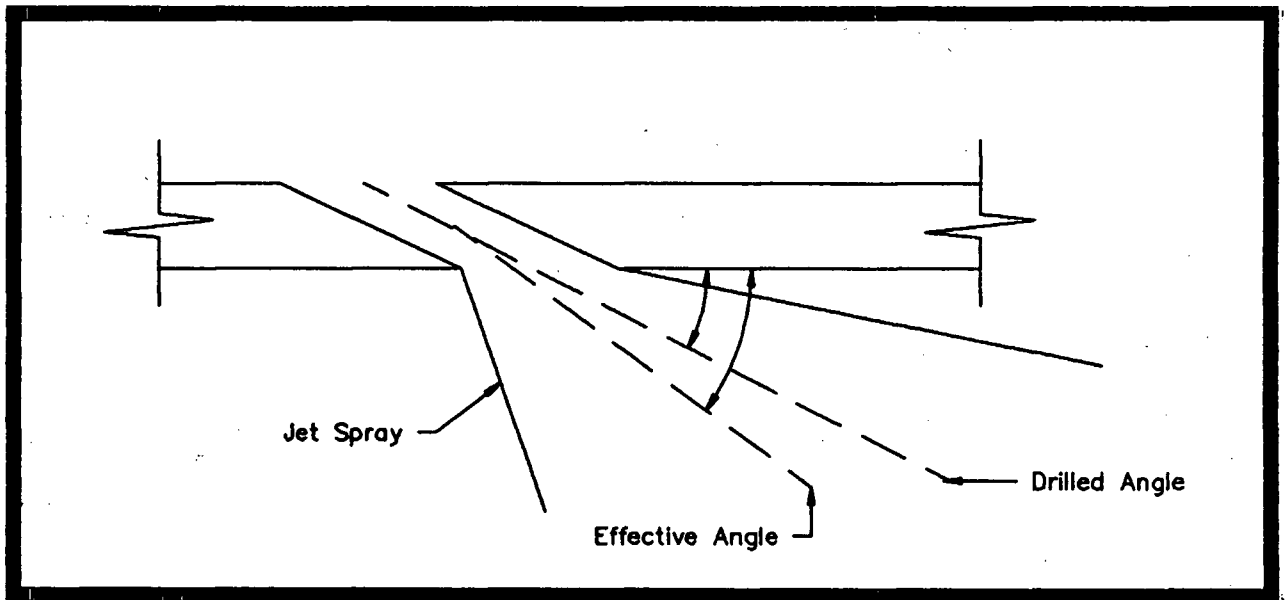


Fig. 8: Drilled vs. Effective Jet Angles

Ring #3.1, the other profile with counter-sunk holes, did not suffer as much deviation as ring #2.1. This may be due to its 19mm wall thickness as opposed to #2.1's 6.4mm thickness. The thicker wall of ring #3.1 permitted for deeper counter-sinking, making for a more controlled jet hole entrance. The jet angle was thought to be better maintained in ring #3.1 than in ring #2.1.

Conclusions

Too much shortening or counter-sinking of the jet hole causes degradation of the jet spray pattern, and the simple one-dimensional theory will not then correlate well with experimental results. The general nature of the jet pump performance can be found, however, various factors will contribute to the randomness of the results. The simple one-dimensional theory sufficiently breaks-down to make performance prediction difficult.

A suggested improvement for the one-dimensional theory is the incorporation of the spread of the jets in terms of reduced momentum in the desired direction. For example, narrow jet spray patterns would have momentum equivalent to $pQ_m V_j$. But wide jet spray

patterns would have momentum equivalent to $K_w \rho Q_m V_j$, where K_w is a coefficient of spray width, having a value less than unity. This suggests that refinement in the one-dimensional theory begins with the reduction of the available momentum in the desired direction. The momentum from wide spray patterns should be factored by a coefficient, K_w , effectively reducing the previously assumed jet momentum. Additional studies in determining how K_w varies with the amount of spray spreading, will be required for this approach to refining the one-dimensional theory.

Jet profiles which do not cause extensive degradation of the spray pattern tend to follow more closely the simple one-dimensional theory. Experiments show that rings, #3.1, #1 and Hillis have better correlation to the one-dimensional theory than rings #2.1, #2 and #3.

3.4 TESTING DIFFERENCES IN JET CONFIGURATION

System Head Tests

Figure 9 shows the jet pump system heads. These plots are required in the selection process of a suitable centrifugal pump source. In conjunction with centrifugal pump curves, the jet pump system head curves can be used for estimating the system operating point. The operating point defines the head and flow at which both the centrifugal and jet pump will operate. Ideally, this point will be optimized for maximum efficiency.

Jet Pump System Heads

For 2.5" Jet Pump, $R = 0.1225$

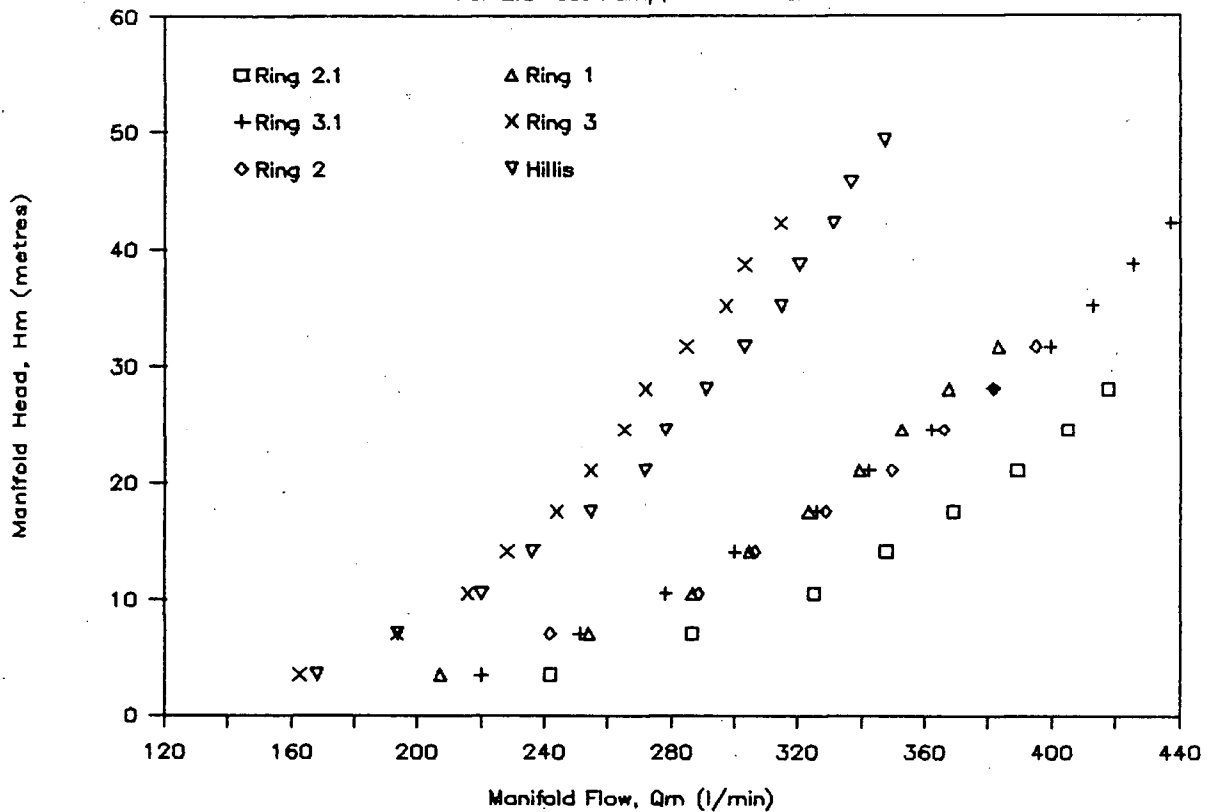


Fig. 9: System Head Curves

Note that ring #2.1 is the flattest curve, indicating the lowest flow resistance. The Hillis ring and ring #3 prove to have the highest flow resistance. Rings 1, 2 and 3.1 all lie within these two bands. Figure 9 tends to support that jet profiles having short relative lengths will have lower flow resistance. This is largely due to the increase in the effective area ratio. Counter-sinking of the jet profile seems to slightly enlarge the jet hole diameter. Therefore, the increase in the area ratio, R , effectively decreases the flow resistance.

Suction Tests

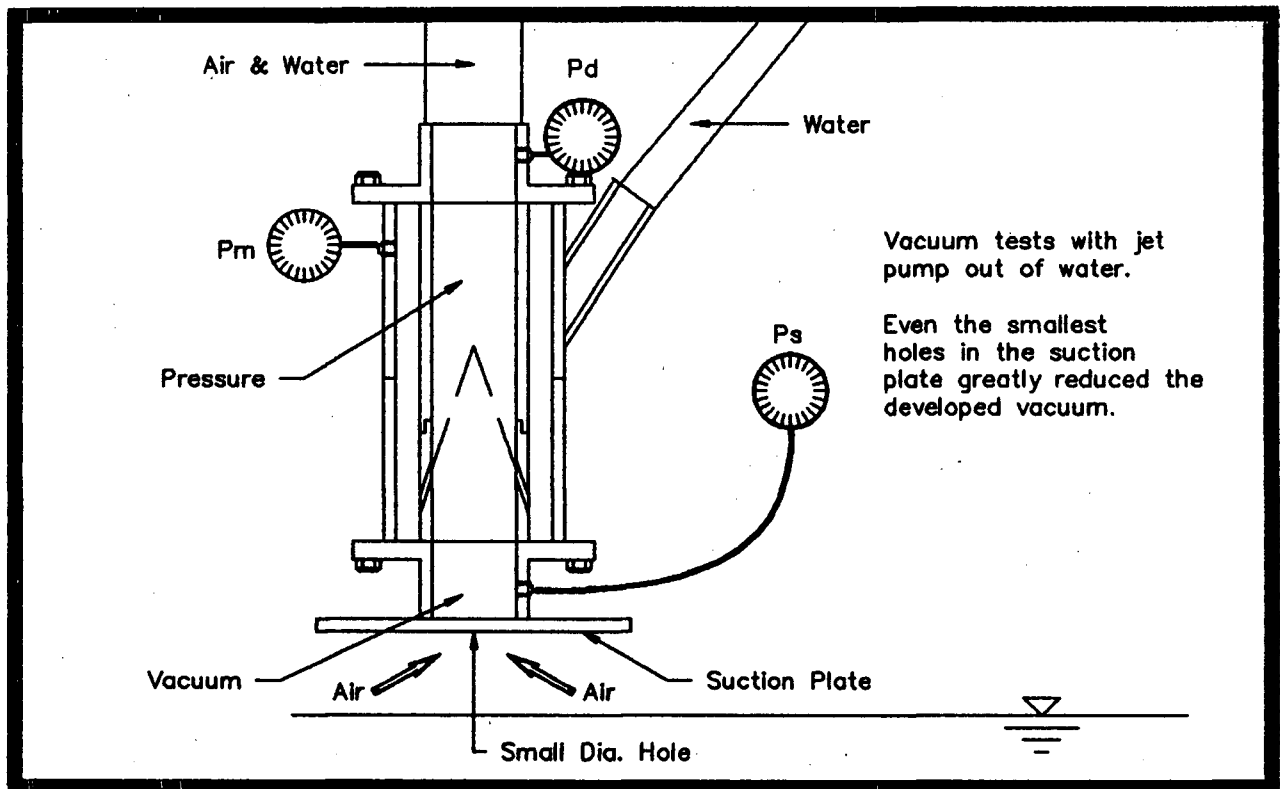


Fig. 10: Vacuum Test Apparatus

Two different suction tests were done. The first test established how the vacuum increased when the front entry of the jet pump was partly closed. For these tests, the jet pump's suction entrance was raised out of the water, operating in the two-phase mode, pumping both air & water. The partial closing of the pump entry was achieved by clamping special perforated plates to the suction entrance. With the hydraulic power held constant, seven different plates with hole diameters varying from 38mm were tried. The developed vacuum was recorded for each plate. Figure 11 shows the plotted results as the developed vacuum vs. the percent closure of the suction entrance.

The second test determined how the developed vacuum varied with the applied manifold pressure. For this experiment, the front opening of the jet pump was fully closed, such that the suction flow, Q_s , equaled zero. The vacuum was successively recorded for each increase in the manifold pressure. Figure 13 shows the results of this test.

First Suction Tests

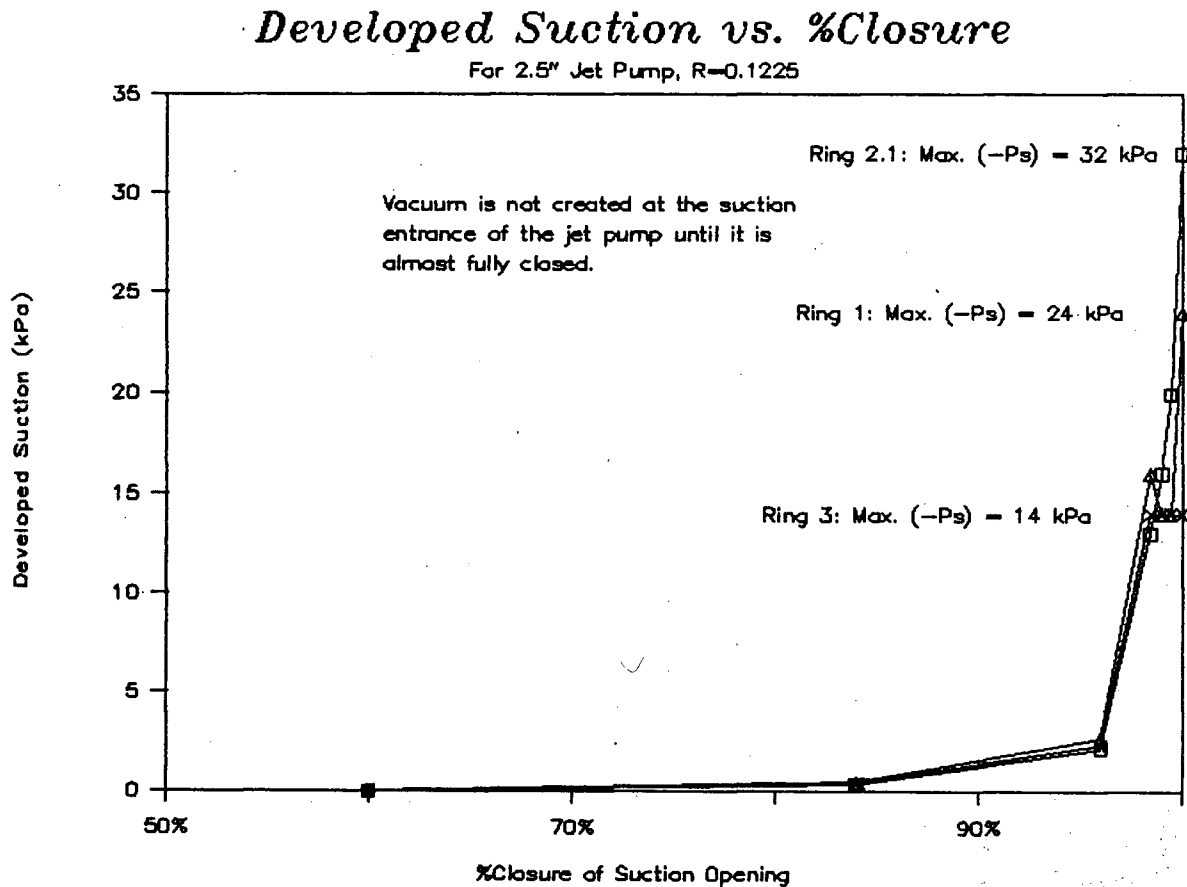


Fig. 11: Variation of Vacuum vs. %Closure

The first suction tests reveal an important factor for proper pumping of liquids. Figure 11 shows that substantial vacuum is not formed at the suction entrance until the blockage of the perforated plates was increased to 96%. This means that the jet pump will not pump liquids effectively until the suction closure is greater than this percentage. Full liquids-pumping capacity is not realized until the suction entrance is 100% closed. Therefore, to maximize liquids pumping capacity, it is important to prevent even the slightest break in the vacuum at the suction entrance.

Furthermore, the tests show that jet rings with shorter relative lengths will develop higher maximum vacuums. Ring #2.1 with R.L. = 2.4, has a maximum vacuum of more

than twice that of ring #3 with R.L. = 8.7. One possible explanation for this phenomena is that the wider spray patterns have greater shear on the surrounding water because, the distributed jet has a large surface area for the development of shear stress. Narrow spray patterns will not share their momentum so quickly or completely and therefore, will produce smaller vacuums.

Air-Pumping Capability

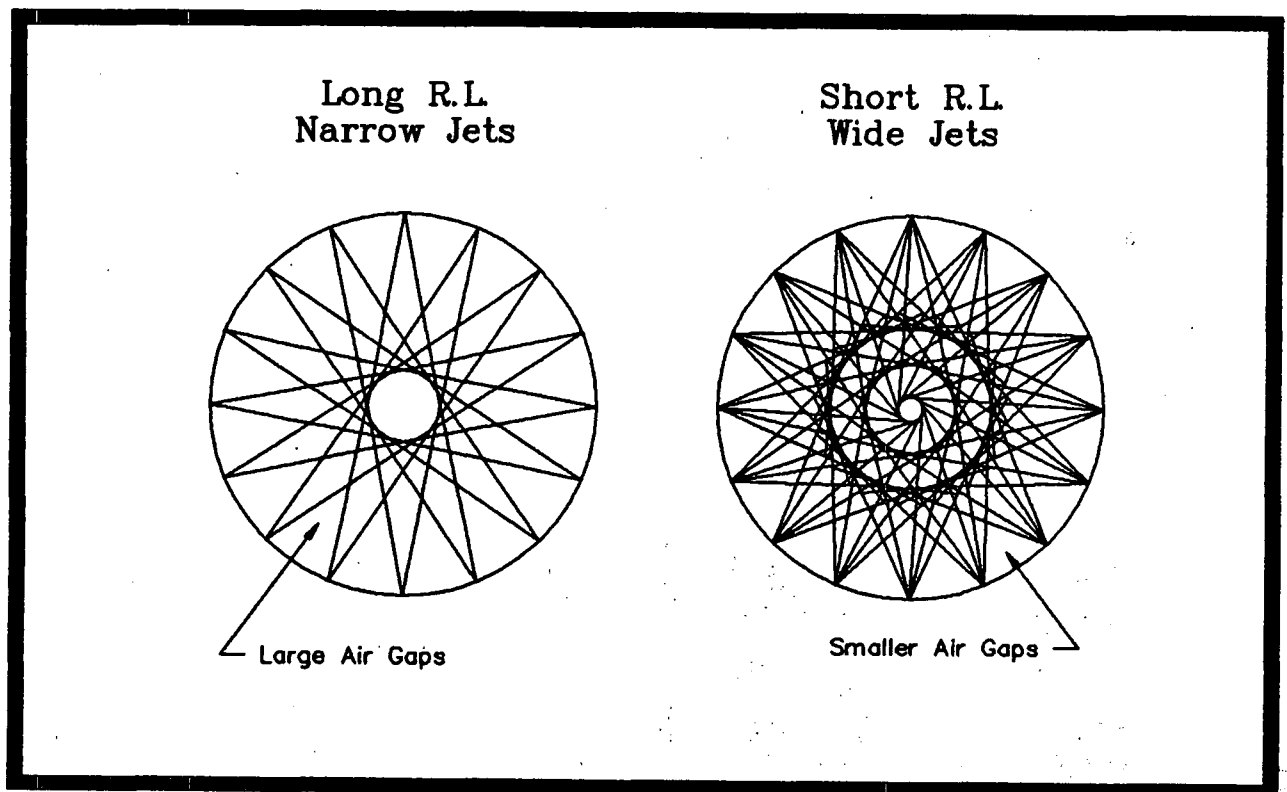


Fig. 12: Air Gaps Between the Jets

Although it was not quantified, shorter R.L. values seemed to have greater air-pumping capacity as well. Long R.L. profiles produce streamline spray patterns which leave larger spaces between the jet spray. If the gap between the jets is large, then the average air velocity passing through the gap is small. As the gap narrows, the average velocity increases. Therefore, wide jets also seem to be better than narrow jets in air-pumping capacity. This behaviour in jet pumps is somewhat analogous to mechanical slip of

conventional air blowers. As the impellers wear, gaps between them widen, reducing the effectiveness of the blower. Similarly, gaps between jets in jet pumps reduce the air-blowing capacity.

Second Suction Tests

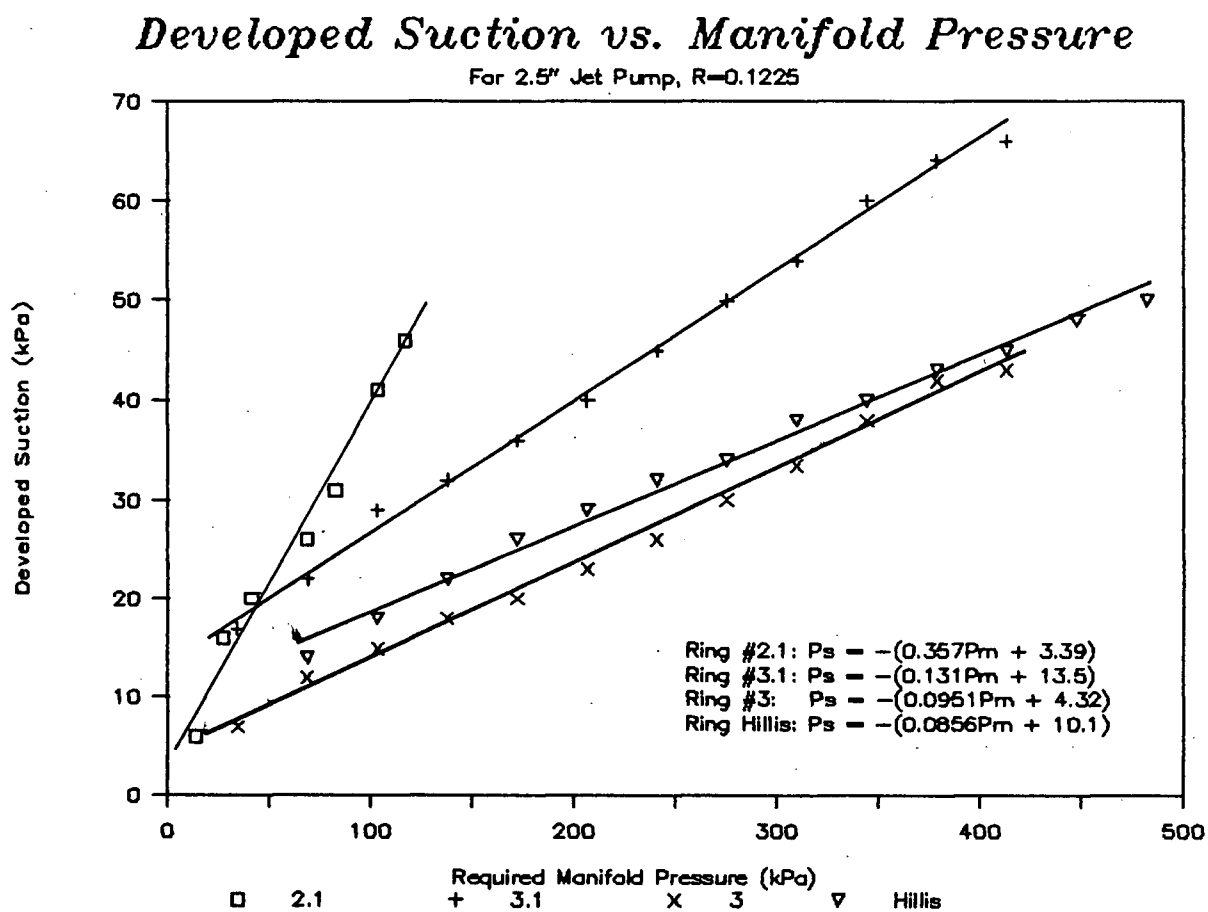


Fig. 13: Variation of Vacuum vs. Applied Pressure

The second vacuum tests disclosed additional differences between the various jet ring configurations (see figure 13). Again, ring #2.1 with its short R.L. showed its superior vacuum-pulling ability. Rings with long R.L. require considerably more manifold pressure to obtain the same vacuum as the rings with the short R.L. For example, ring #3 needs about 270kPa to achieve 30kPa of suction, while ring #2.1 needs only about 75kPa.

During the vacuum tests, one common feature was observed. When the various plates were clamped over the suction entrance, the vacuum did not develop immediately. It often took a few seconds until the needle on the gauge rose to its maximum reading. It was found repeatedly, that the rise in vacuum corresponded to the "filling-up" of the area in the suction entrance. Once the suction entrance area was full of water, the jets sprayed into water instead of air. At this point in time, the needle on the gauge deflected to its maximum reading. It is thought that the shear on the water by the jets attributed to this behaviour.

This observation shows the importance of placing the jets near the suction entry. For example, if the jets were remotely located from the entry, it would take a longer time to fill the suction area with water. This means that a good vacuum will not develop, and subsequent performance will be poor until this area is filled. Having the jets closer to the entry will shorten the time required until good performance is achieved.

Conclusions

Both the system head tests and suction tests demonstrate the differences in the characteristics for the various jet profiles. Given the same area ratio, R , short relative jet lengths produce less head and greater vacuum, while long relative jet lengths produce more head and less vacuum. If vacuum is the criterion, this implies that long relative lengths are inferior to short relative lengths (ring #3 has a long R.L.).

However, when the relative length becomes too short, the jet spray pattern widens. This degrades the spray sufficiently that it effectively increases the drilled hole diameter. Subsequently, the effective spray angle deviates from that of the original drilled angle. In addition, as the spray pattern widens, the momentum produced by the jet decreases. As previously stated, improvements in the one-dimensional theory by incorporating a coefficient of spray width, K_w , to the jet momentum may resolve this discrepancy between experiment and theory. But until further investigation is done, existing jet profiles with excessively

short R.L. will be difficult to predict by the current one-dimensional theory (ring #2.1 is an example).

Jet Ring Performance Summary

Ring Ref. #	R.L.	Correlation With Theory	Suction Performance	Head Performance	Overall Performance
2.1	2.4	4	1	4	9
3.1	2.5	1	2	3	6
2	3.4	2	3	3	8
Hillis	3.4	2	4	2	8
1	6.9	1	5	3	9
3	8.7	3	5	1	9

Summary of the suction and head performance of the various rings are given in the table above. They are ranked in the order from best to worst, with a value of 1 for the best performance. The actual performance numbers are arbitrary, but rings having similar performance were given the same rating. For example, the best suction performance was from ring #2.1, the best head performance from ring #3, and the best overall performance from ring #3.1.

Depending on whether the criterion for performance is suction, head, or a combination of both, a good design can be established using the guidelines set here. In general, for good suction capability, jets should be designed with short relative jet lengths. For good head performance, jets should have long relative jet lengths.

3.5 TESTING FOR SOLIDS-HANDLING CAPABILITY

Quantitative measurements were not taken for any of the solids-handling tests. Only qualitative observations were made. Two general tests were done using ring #3.1 and the apparatus similar to that in figure 5.

Point of Solids Injection

When pumping solids through the jet pump, the location at which the solids are introduced into the system is important. In other words, the location of the jets with respect to the solids has a significant effect on how the solid passes through the system. This is true if the jet pump is submerged below the water surface, and critical if the jet pump is unsubmerged above the water surface. A small piece of wood 100mm long was used to observe the pumping action. For tests in the submerged state, the suction entrance was extended with a 300mm long hose to exaggerate the distance to the jets (see figure 14).

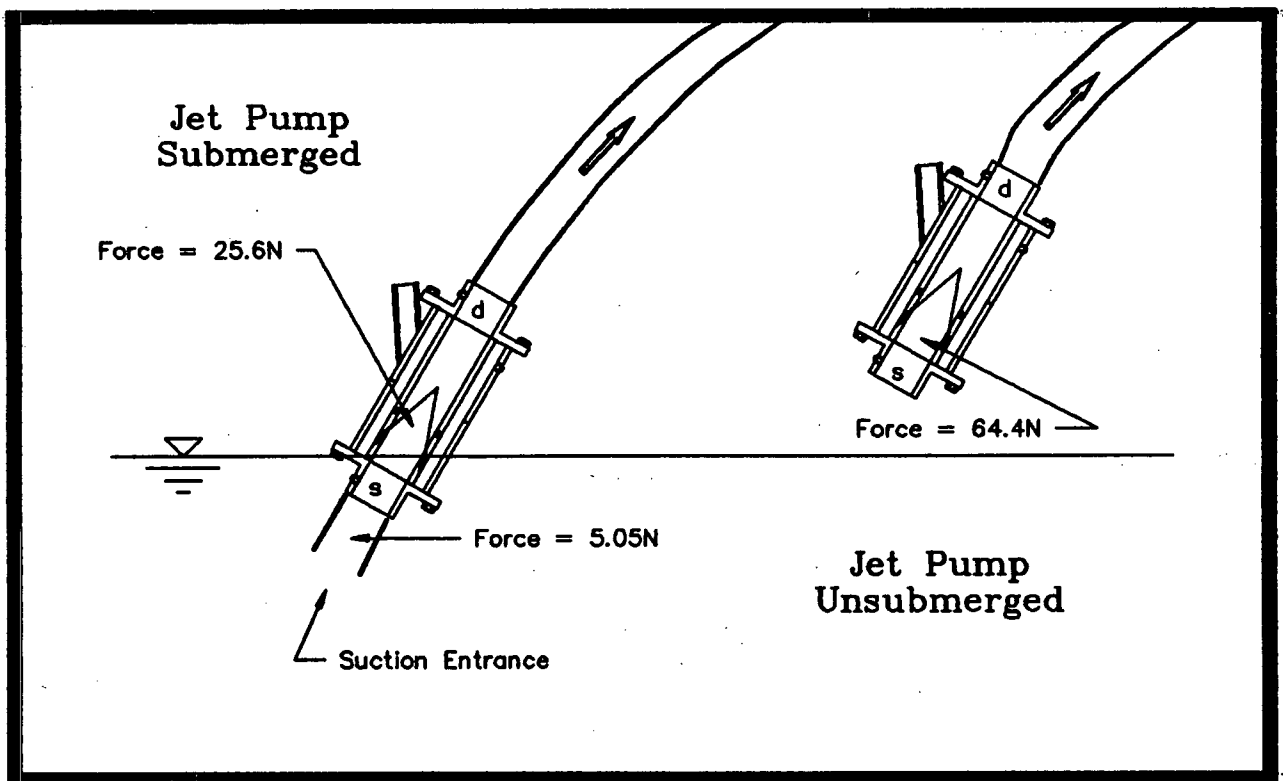


Fig. 14: Point of Solids Injection

Jet Pump Submerged

With the jet pump in the submerged state, the piece of wood was held and released from two locations. The first location was at the suction entrance, and the second location was right at the jet location.

The entrainment of solids at the suction inlet depends on the force exerted at this section. Once the solids are entrained, they will undergo rapid acceleration when they reach the jets. The reasoning can be explain by the hydraulic force-momentum principle. For the submerged condition, if the solids are introduced prior to the jets, the momentum forced onto the solids will be $pQ_s V_s$. If the solids are introduced right at the jet location, then the momentum would be $p(Q_s + Q_m)V_d$. In other words, the force exerted onto the solids will be much greater if the solids are introduced at the jet location. For example, assuming a flow ratio, $M = 0.8$, suction area, $A = 0.00317\text{m}^2$, area ratio, $R = 0.1225$, and a manifold flow, $Q_m = 300 \text{ l/min}$:

$$Q_s = Q_m M = 240 \text{ l/min} = 0.004\text{m}^3/\text{s}$$

$$Q_d = Q_s + Q_m = 540 \text{ l/min} = 0.009\text{m}^3/\text{s}$$

$$\text{suction force} = pQ_s V_s = \underline{5.05\text{N}}$$

$$\text{discharge force} = p(Q_s + Q_m)V_d = \underline{25.6\text{N}}$$

The above calculation shows that the momentum exerted on the solids by the water is far greater at the jets than at the suction entrance.

Jet Pump Unsubmerged

For the unsubmerged case, the suction hose extension was removed before the test. As expected, the jet pump could not pick-up the piece of wood unless it was thrown into the jets. Once in contact with the jets, the wood was carried away at speeds much greater than that in the submerged state. Again, using the same example, the momentum at the jets can be estimated:

$$A_j = AR = 3.88 \times 10^{-4} \text{ m}^2$$

$$Q_m = 300 \text{ l/min} = 0.005 \text{ m}^3/\text{s}$$

$$\text{jet force} = p Q_m V_j = \underline{64.4 \text{ N}}$$

An overwhelming 64.4N of hydraulic force is available at the jets in the unsubmerged state. Compare this to 25.6N for the submerged state. This example shows the importance of where the solids are introduced into the system.

Submergence of the Suction Entrance

The solids-pumping ability was also dependent on the location of the suction entrance. For solids suspended in water, the jet pump could be operated in the submerged state. But for floating solids, if the inlet is tilted so that about 95% of the suction entrance area is below the water surface, then even greater solids-handling capacity was achieved. This behaviour tends to support the previous findings on developed suction and percent closure (refer to figure 11).

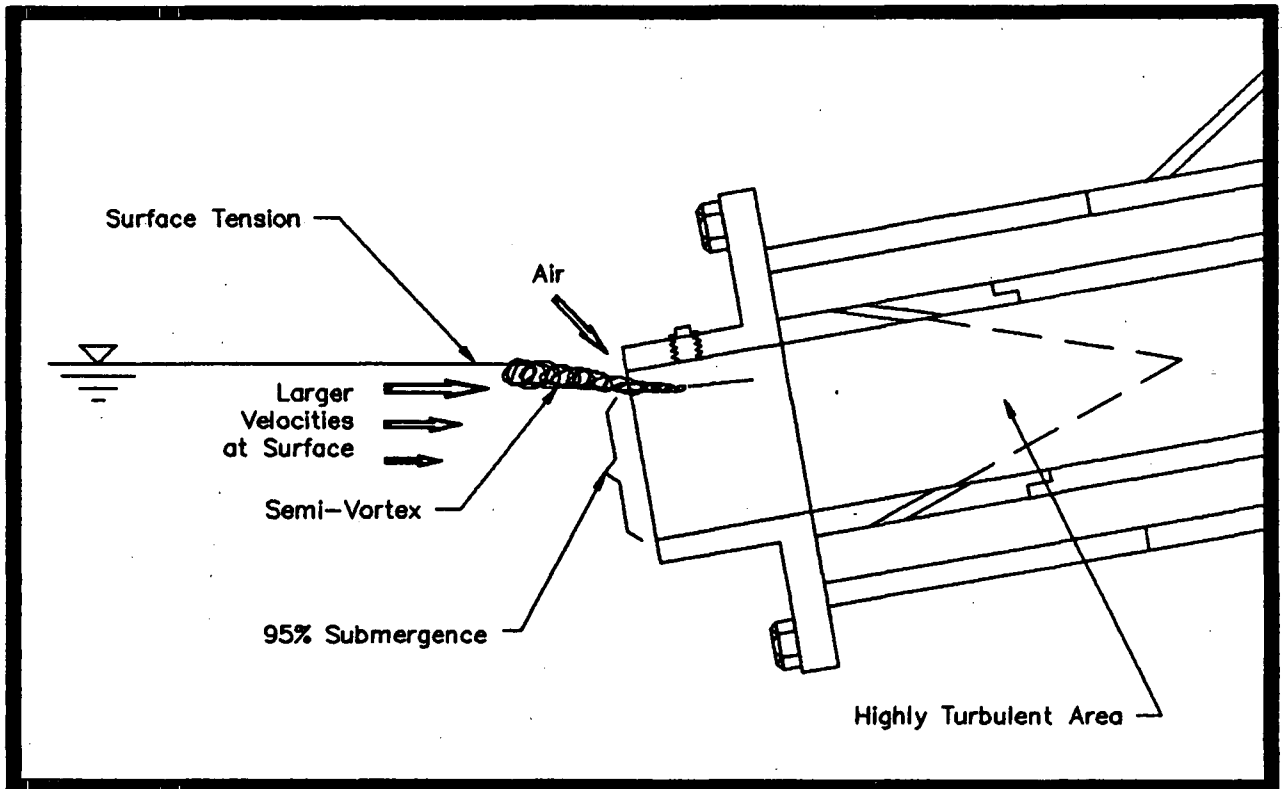


Fig. 15: Partial Submergence

When operated at 95% submergence, the jet pump makes "gurgling" sounds as it forms and reforms vortices at the suction entrance. In conjunction with surface tension, the vortices actually help to draw the floating solids into the suction entrance. As the jet pump pulls on the surface tension, it brings with it the solids which cling to it.

Conclusions

When the desired goal for the jet pump is to move solids, then it must be determined where the solids are to be introduced into the system. It should also be determined if the jet pump is best suited for submerged, unsubmerged or partially submerged operation.

For transporting unbreakable solids, it may be best to position the jet pump out of the water, and then mechanically feed the solids to the jets. This will ensure the application of the maximum force on the solids by the jet pump (64.4N in the example). If the solids are

more fragile, then the jet pump should be submerged. When the solid first reaches the jets, a momentum will be exerted on it (25.6N in the example). This will provide a more gentle handling action. For an even more gentle action, an extension suction hose can be added to the suction inlet, where the exerted force will be smallest for the entire system (only 5.05N in the example).

Air and solids entraining vortices were natural occurrences when the jet pump was operated in the partially submerged state. Floating solids were entrained into the vortex and along with some drawn air, were swept away into the suction inlet. Some of the jet pump's best solids-handling abilities were observed with the jet pump in this partially submerged state.

4. APPLICATIONS IN FISH TRANSPORT

Four prototypes of fish pumping systems were built during the two years after tests were completed in the laboratory. One of each of the following sizes were manufactured: 101.6mm (4inch), 152.4mm (6inch), 203.2mm (8inch) and a 254mm (10inch). Various tests were carried out as described in the next sections, but the opportunity to test each one as thoroughly as the laboratory model was not possible. The prototypes were owned by customers who pre-paid for the manufacture of the jet pump, and they wished to have them shipped as soon as possible.

Some of the findings from the laboratory model were transferred to the prototype jet pumps. For example, the jet ring profiles for all the prototypes were modeled from ring #3.1. The advantages of ring #3.1 were in its more predictable hydraulic behaviour, yet it had nearly the same vacuum-pumping capacity as ring #2.1.

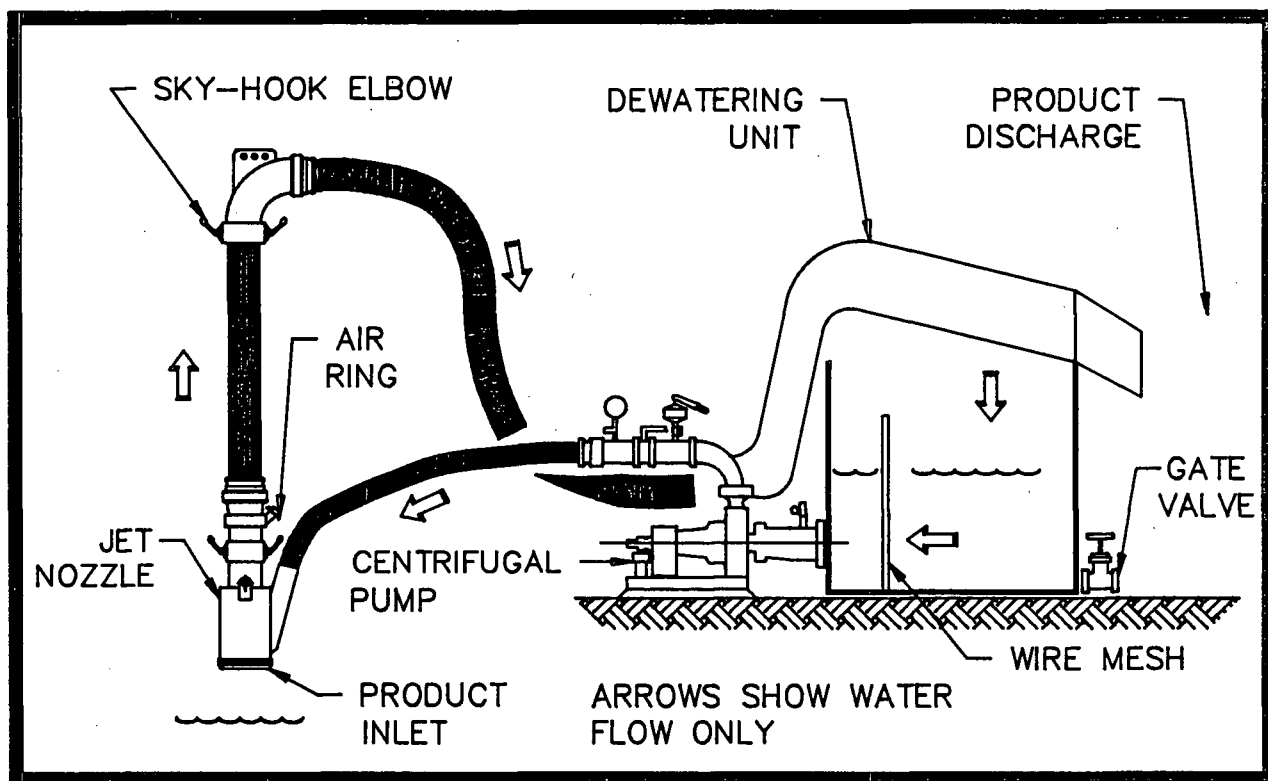


Fig. 16: A Prototype Fish Pumping System

Limited pumping of live salmon smolts were also tried with the 101.6mm prototype. With the existing design, some small percentage of the smolts were either killed or damaged. Further work would be needed to redesign and test pumps for this purpose.

4.1 SYSTEM ANALYSIS

In chapter 2, a simple one-dimensional theory for the intrinsic operation of the jet pump was derived. The result given by equation [2.18] gives the jet pump characteristic, analogous to pump curves given by reputable pump manufacturers. But, like any exercise in pump selection, a system analysis must be done before the pump curves can be matched.

A system analysis for general applications will be examined. The generalization of the system curve will make it simple to customize it for any application, whether it be for a fish pump, crab pump or a ship's bow thruster.

Figure 17 shows the general set-up for the jet pumping system. For the purposes of this analysis, the suction flow, Q_s , is assumed to be always positive. This will rule-out the case when the lifting height, $(Z_c - Z_s)$, is too high such that back-flow occurs. Continuity and Bernoulli theorems will be used.

The Head Ratio Definition (Revisited)

Attempts were made to write the system curve in a non-dimensional form, using the basic definition given in equation [2.2]:

$$N = \frac{H_d - H_s}{H_m - H_s} \quad [2.2]$$

These attempts were partially successful, but result in a family of curves, each with a different manifold flow, Q_m , or lifting height, $(Z_c - Z_s)$. Using energy methods, the head terms can be substituted with pressure, velocity and height terms.

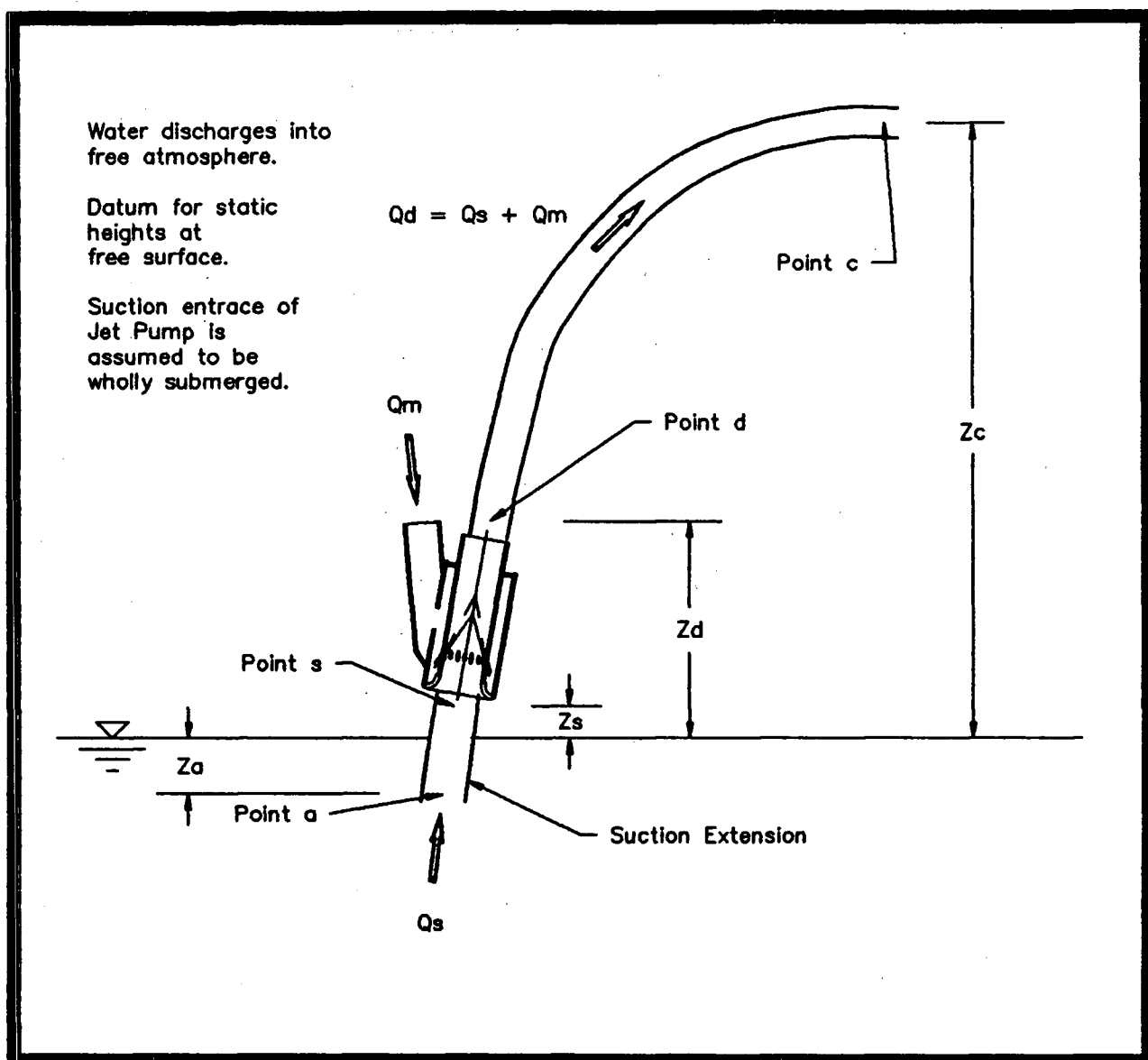


Fig. 17: System Analysis

Bernoulli Theorem

Applying between points d & c:

$$H_d = \frac{V_c^2}{2g} + \frac{P_c}{pg} + Z_c + H_{lc} \quad [4.1]$$

Where H_{lc} is the sum of the head losses between d & c.

Applying between points a & s:

$$\frac{V_a^2}{2g} + \frac{P_a}{pg} + Z_a = H_s + H_{ls} \quad [4.2]$$

Applying between points m & s:

$$H_m = \frac{V_j^2}{2g} + \frac{P_s}{pg} + Z_s + K_2 \frac{V_j^2}{2g} \quad [4.3]$$

Where H_{ls} is the sum of the head losses between a & s, and K_2 is the head loss coefficient for the manifold and jets. Then substitute equations [4.1], [4.2] and [4.3] into [2.2]:

$$N = \frac{\frac{V_c^2}{2g} + \frac{P_c}{pg} + Z_c + H_{lc} - \frac{V_a^2}{2g} - \frac{P_a}{pg} - Z_a + H_{ls}}{\frac{V_j^2}{2g} + \frac{P_s}{pg} + Z_s + K_2 \frac{V_j^2}{2g} - \frac{V_a^2}{2g} - \frac{P_a}{pg} - Z_a + H_{ls}} \quad [4.4]$$

Equation [4.4] defines the general system curve equation for the example shown in figure 17. From here, additional analysis must be done to express the velocity terms as functions of flow, either Q_s or Q_m . Individual cases for each jet pump application will help to simplify this equation.

For example, in fish pump applications, the suction extension is usually not used. Therefore, in equation [4.4], $V_a = V_s$, $P_a = P_s$, and $Z_a = Z_s$. Additionally, by energy, $P_s/(pg) = -V_s^2/(2g)$. The sum of the head loss between a & s, H_{ls} , would be reduced to an entrance loss = $K_s V_s^2/2g$. Where K_s is a loss coefficient, usually taken as 1. The system usually discharges into atmospheric air, thus, $P_c = 0$. Equation [4.4] becomes:

$$N = \frac{\frac{V_c^2}{2g} + Z_c + H_{lc} - Z_s + K_s \frac{V_s^2}{2g}}{\frac{V_j^2}{2g} + K_2 \frac{V_j^2}{2g}} \quad [4.5]$$

Assuming that the discharge hose diameter is the same as that of the jet pump discharge, $V_c = V_d$. Then using continuity, $V_d = (Q_s + Q_m)/A$, $V_j = Q_m/(AR)$, $V_s = Q_s/A$. $H_{lc} = K_{lc} V_d^2/(2g)$, assuming that all the discharge head losses can be expressed as a function of the discharge velocity, V_d . K_{lc} is the sum of all the discharge hosing loss factors. Substituting for [4.5]:

$$N = \frac{(1+K_{lc}) \frac{(Q_s + Q_m)^2}{2gA^2} + (Z_c - Z_s) + K_s \frac{Q_s^2}{2gA^2}}{(1+K_2) \frac{Q_m^2}{2g(AR)^2}} \quad [4.6]$$

Fish Pump System Curve Equation

Another form of the system curve is derived if the definition of M , as given in equation [2.1] is substituted:

$$N = \frac{(1+K_{lc})(M+1)^2 + K_s M^2 + \frac{2gA^2(Z_c - Z_s)}{Q_m^2}}{\frac{(1+K_2)}{R^2}} \quad [4.7]$$

Unfortunately, the system curve for fish pumping applications can not be made dimensionless. This is due to the hydraulic lift height term, given by $(Z_c - Z_s)$. For fish pump applications not requiring lift, the system curve equation could be plotted together with the pump curve equation [2.18], on the same non-dimensional N - M graph. The intersection of [4.7] and [2.18] defines the system operating point for the jet pump. This would solve for the operating point graphically.

An analytical solution is also possible. Equation [4.7] can be subtracted from equation [2.18], effectively eliminating the variable, N . If the lifting height, $(Z_c - Z_s)$, is assumed to be fixed, two unknowns, M & Q_m will remain. Solving for M , given Q_m , or vice versa will give

one parameter of the operating point. The other parameter, N , is found by recalculating [4.6] using the new values for Q_s and Q_m , knowing that $Q_s = MQ_m$.

4.2 EXPERIMENTAL PROCEDURES

Although time for testing the prototypes was limited, four basic tests were performed on the jet pumps. These are:

- 1) System Head Tests: Determines the Head & Flow characteristics. Gives indication of correct manifold & jet hole sizing. Also provides information to correctly assess the required size of the centrifugal pump.

Procedure: Increase manifold pressure, P_m , and record the corresponding manifold flow, Q_m . Use the recorded pressure & flow to plot a system curve.

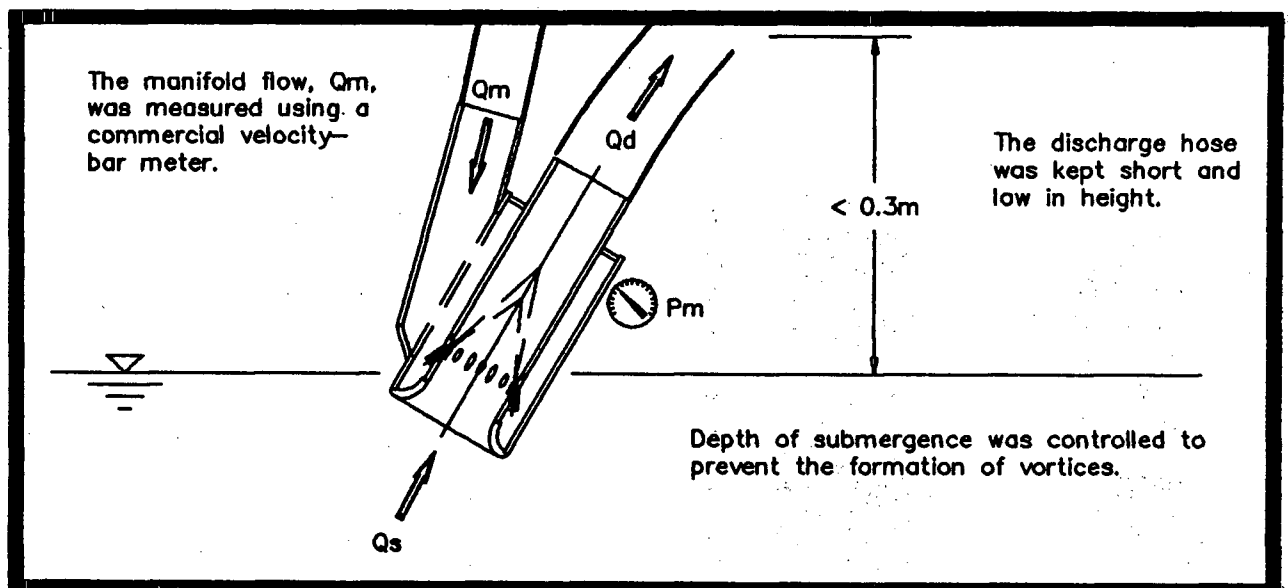


Fig. 18: System Head Test

- 2) Suction Head Tests: Determines the vacuum-pulling capability of the jet nozzle.

Indicates whether or not the jet hole profile is correct. Affects ability to develop good intake suction.

Procedure: Clamp acrylic board over the jet pump suction entrance. Increase manifold pressure, P_m , and record the developed vacuum, P_s . Also, record the manifold flow, Q_m , for reference. A graph of vacuum vs. manifold pressure, should produce a near linear graph.

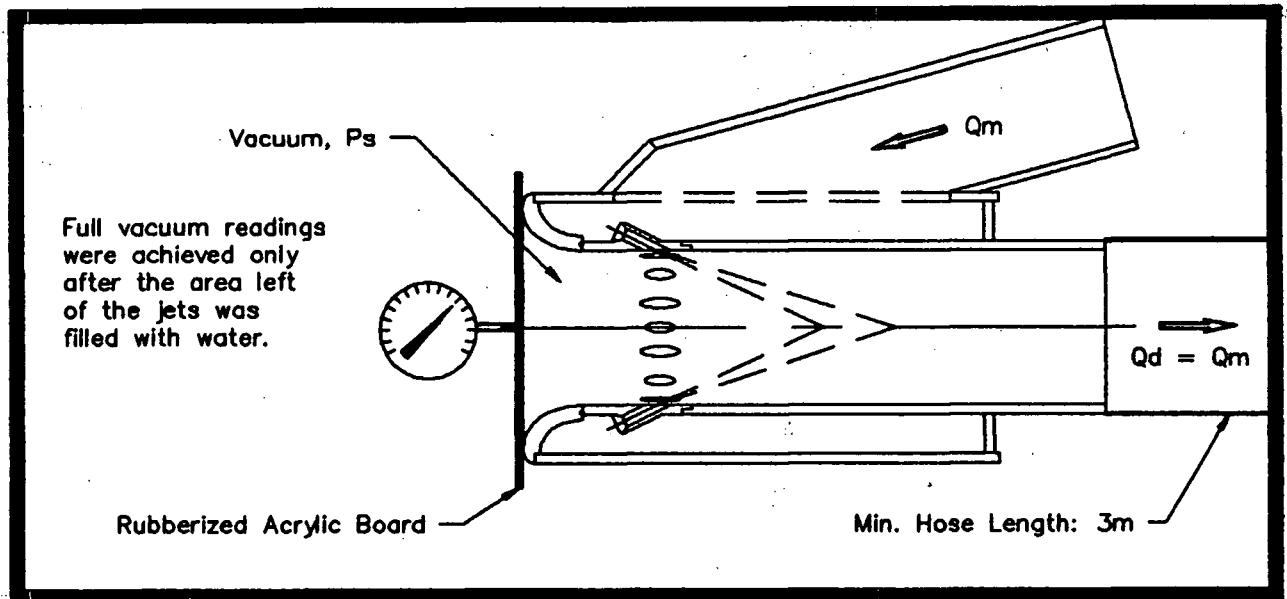


Fig. 19: Suction Head Test

3) Static Lift Tests: Indicates potential lifting ability. Gives total energy input into the system, via P_d measurements.

Procedure: Connect a clear hose to the jet pump discharge, and hold upright as a stand pipe. Progressively increase P_m , and record the Q_m and static lift height. When the static height is plotted against the manifold pressure, a linear relationship results.

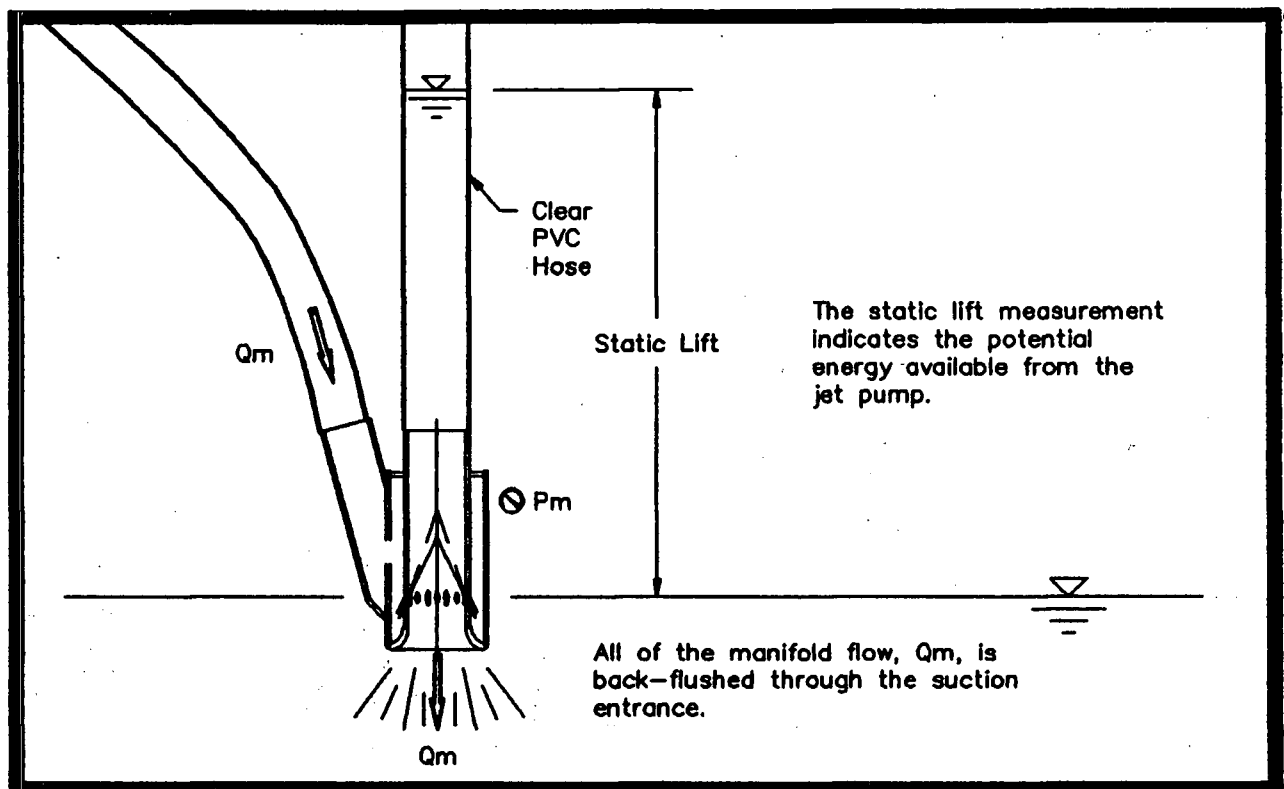


Fig. 20: Static Lift Test

- 4) Qualitative Dynamic Lift Tests: Final inspection of system to determine its ability as a fish pumping system.

Procedure: Lower discharge hose until sufficient pumping action is achieved through jet pump. Ascertain correct pumping action by inducing solid specimens through the system. Operate the pump in both the submerged and non-submerged conditions.

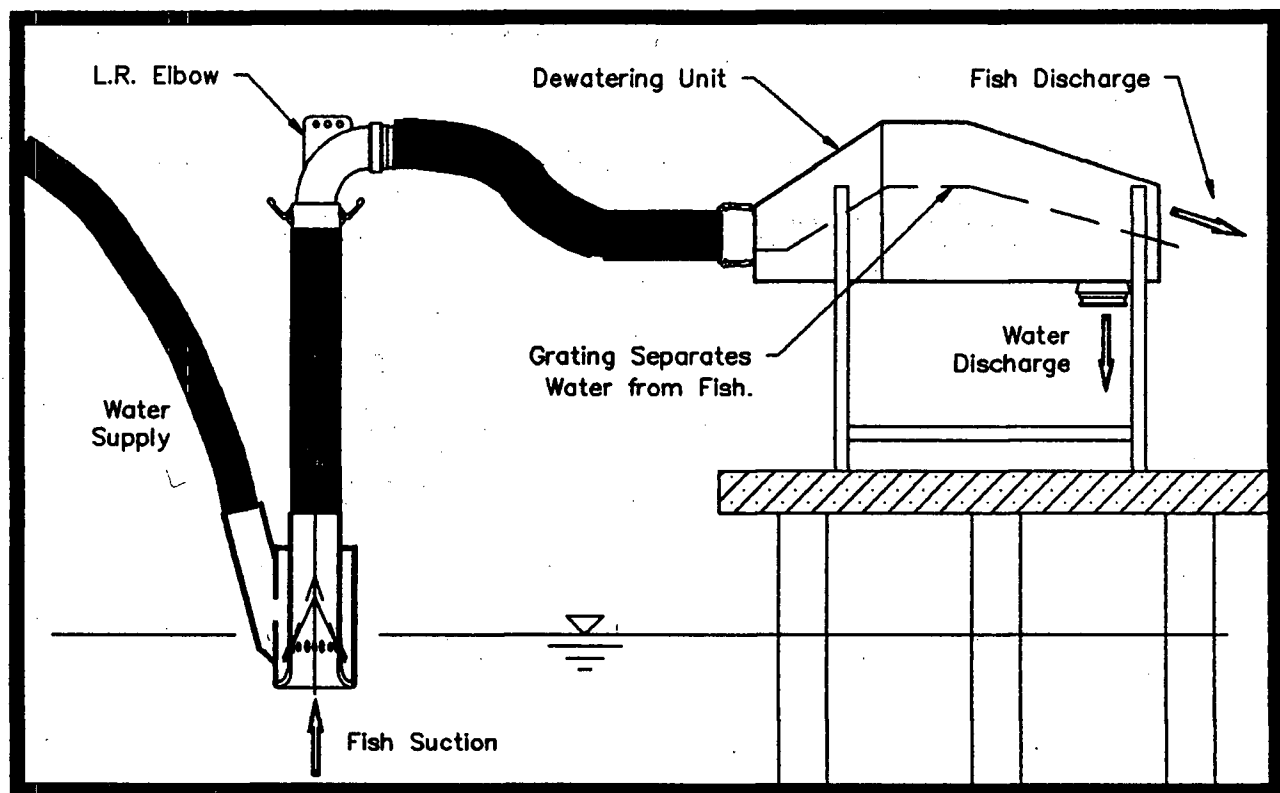


Fig. 21: Dynamic Lift Test

4.3 RESULTS

System Head Tests

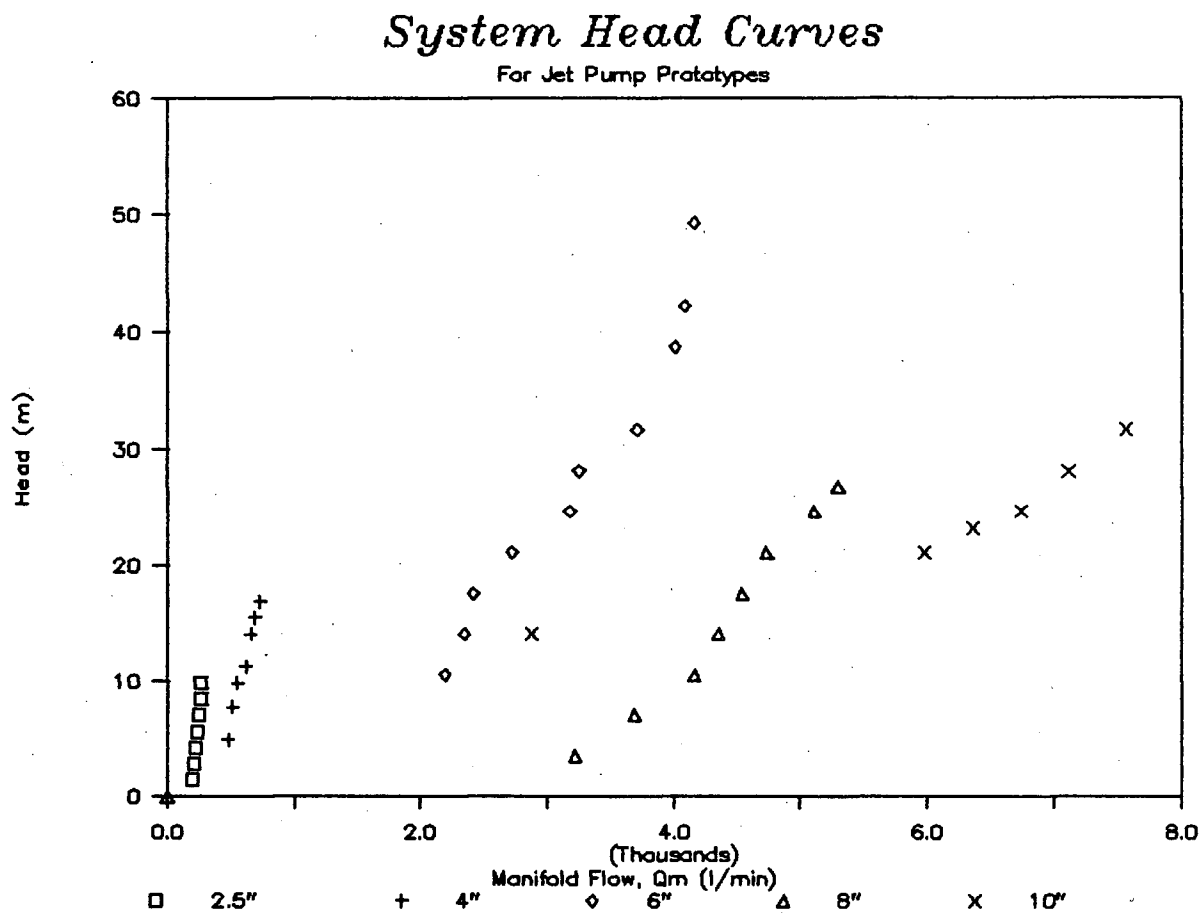


Fig. 22: System Heads

As expected, figure 22 shows the larger jet pumps requiring greater flow capacities. All of the prototypes were designed with similar operating heads, at about 30m. Limitations in the testing equipment restricted the measured range for the various prototype sizes as shown. The 63.5mm (2.5") prototype is the actual data from the laboratory model with ring #3.1.

Suction Head Tests

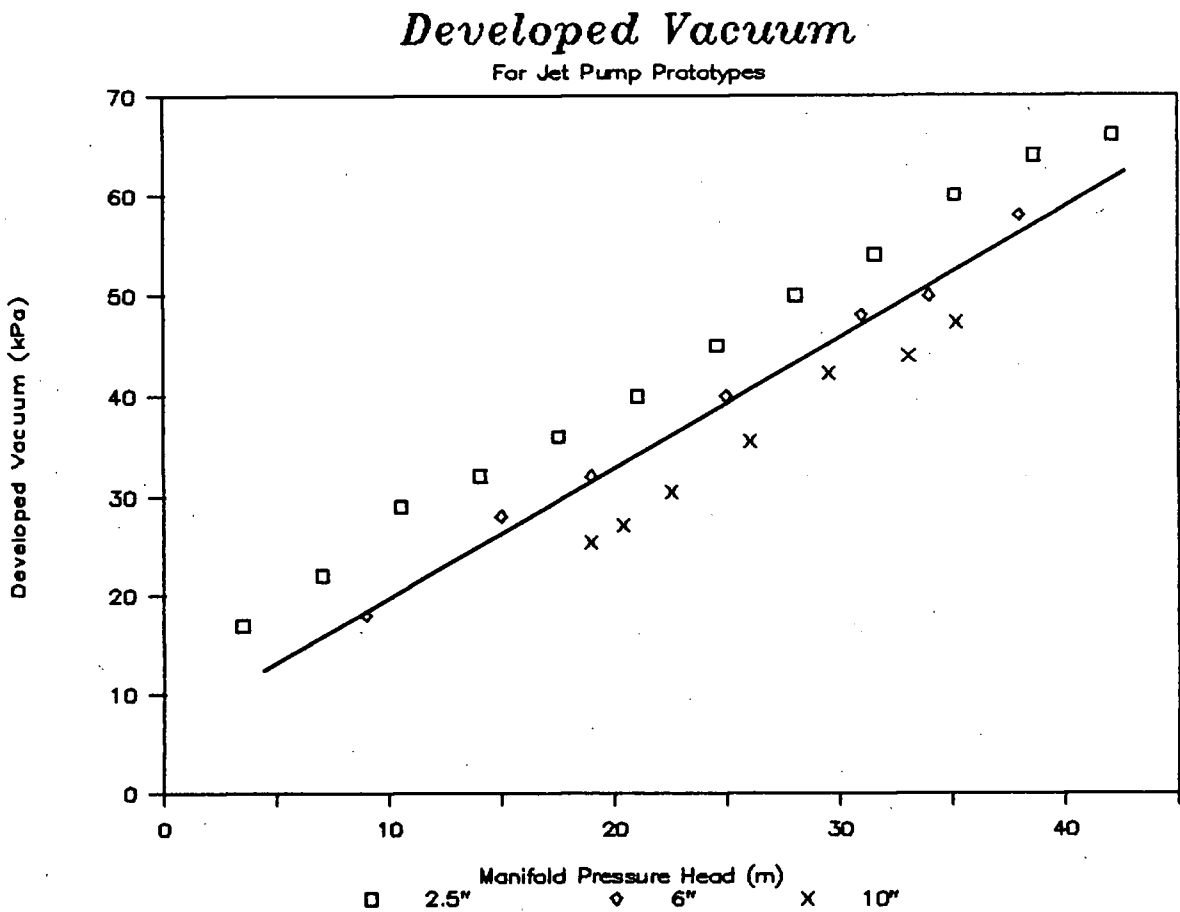


Fig. 23: Suction Heads

For all prototypes having area ratio, $R = 0.098$, the suction heads created at P_s , is essentially linear with the manifold pressure. This shows the variability of the effects of scaling to the larger sizes. If the scaling were perfect for the jet pumps, then all the points for each of the jet pumps would be coincident. Only one line would emerge for all jet pumps having $R = 0.098$.

By linear regression, the averaged relationship yields:

$$-P_s = 1.33 P_m/(pg) + 6.7 \quad [4.8]$$

where P_s is given in kPa and $P_m/(pg)$ is given in metres.

In theory, each line should initially be linear, passing through the origin, and coincident with the other prototypes. Eventually, as the vacuum continues to increase, the full-vacuum maximum will be approached. The line will then become non-linear, and any further increases in the manifold pressure will not increase the developed vacuum.

Static Lift Tests

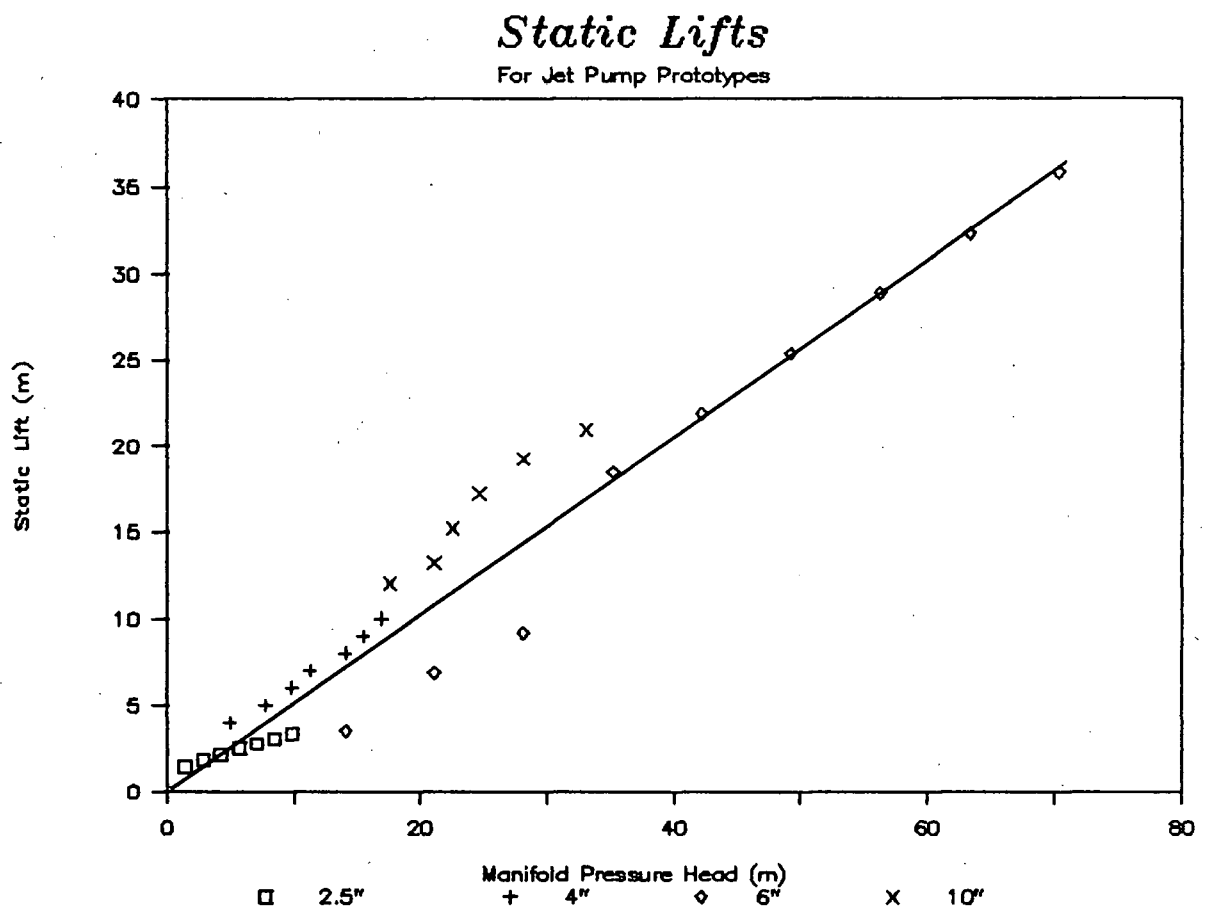


Fig. 24: Static Lifts

Figure 24 shows the variability of the static lifts for the jet pump prototypes. Again, ideally all the lines should be linear, coincident, and passing through the origin.

The averaged linear regression for all the data points is:

$$(Z_c - Z_s) = 0.53 P_m / (\rho g) \quad [4.9]$$

where $(Z_c - Z_s)$ and $P_m / (\rho g)$ is in metres.

This graph shows that regardless of the jet pump size, if the area ratio, R , is fixed, then the same manifold pressures should result in similar static lifts. This makes it simple to scale static lift performance for prototypes of different size, but having the same area ratio.

Dynamic Lift Tests

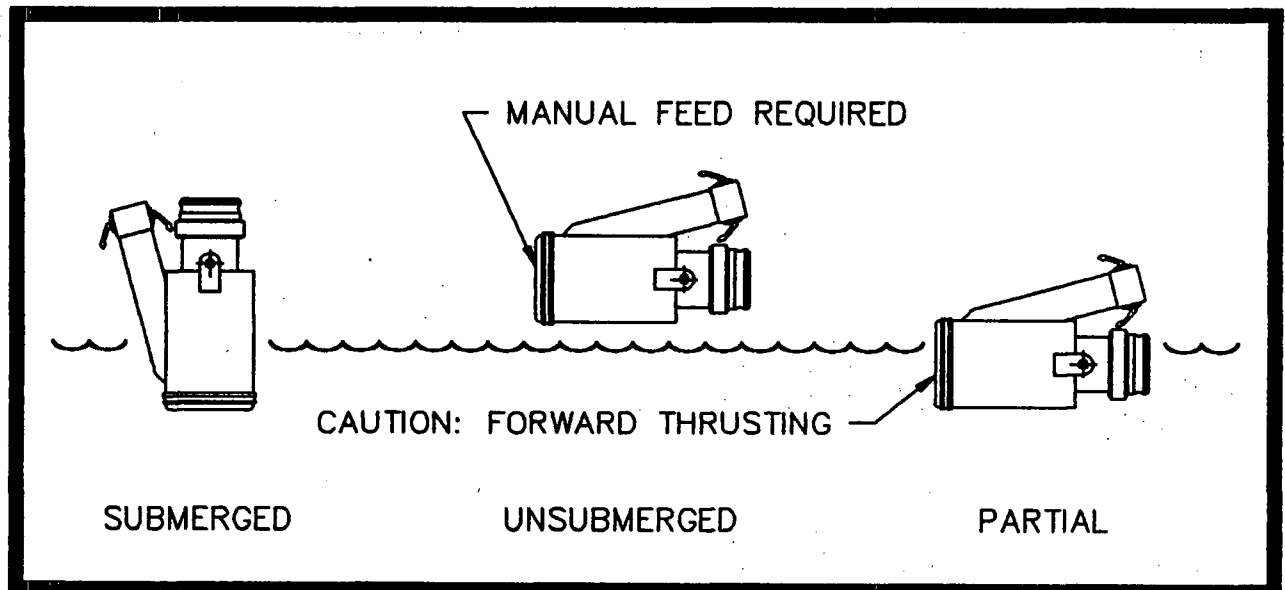


Fig. 25: Submerged, Unsubmerged & Partial Operation

When the jet pump was operated in the submerged and unsubmerged condition, without solids, the flow through the system was steady. However, when the jet pump was operated in the partially submerged condition, the flow became non-uniform. The jet pump sometimes entrained more suction fluid than usual, sometimes less. This often lead to surging, or thrusting of the jet pump, since the amount of momentum transferred was not

constant. It is unlikely that any theoretical relationship can predict this non-uniform performance.

When live salmon smolts were tested as specimens, some problems did arise. Loss of scales, damage to the eyes, and bleeding behind the gills, were some of the casualties the salmon suffered. It appeared that the momentum from the jets were too strong and concentrated, such that damage to the salmon was unavoidable. In future designs, distribution of the momentum through increasing the number of jet holes is recommended. Clearly, there is a need for additional research in this area.

5. APPLICATIONS IN A CRAB SAMPLING DEVICE

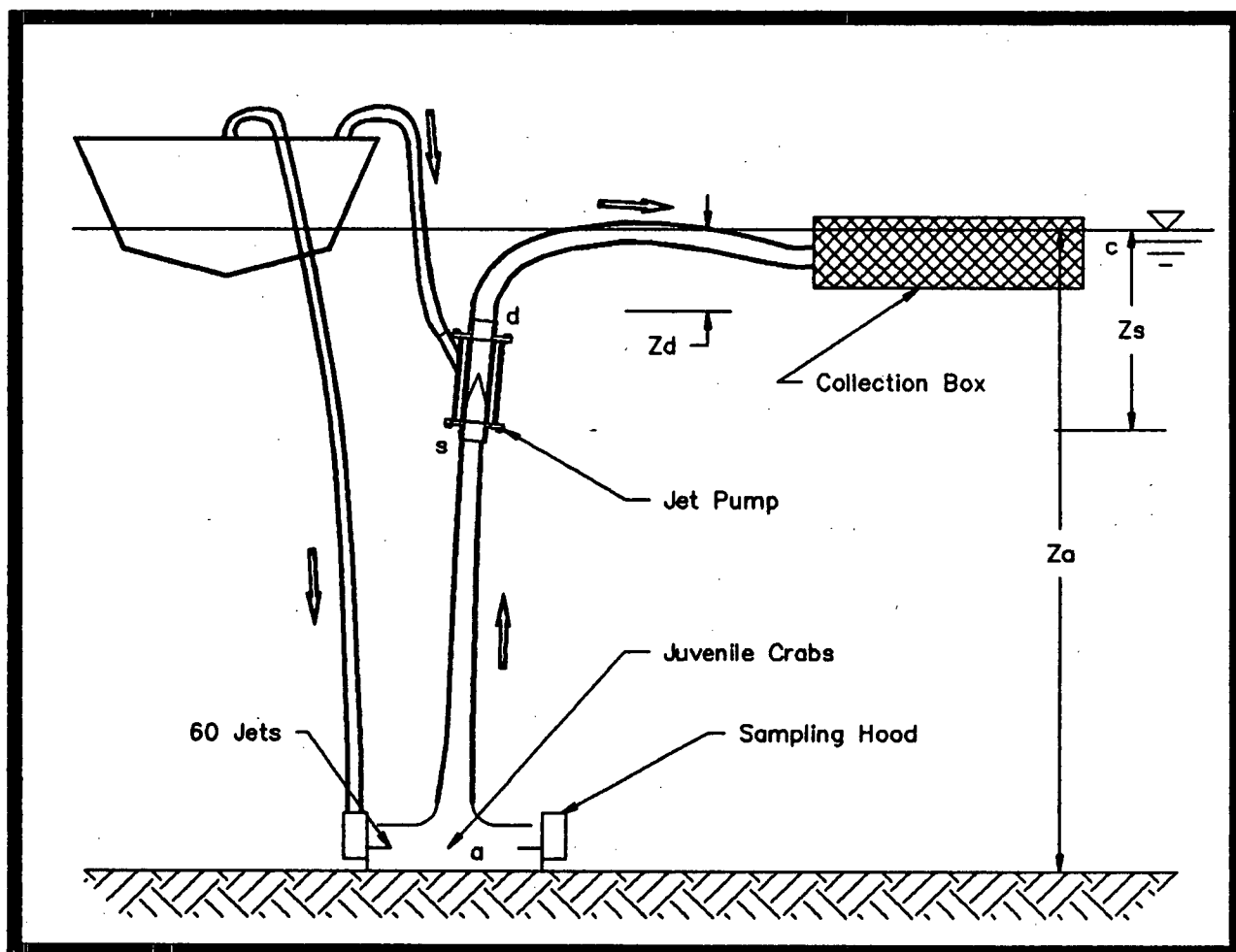


Fig. 26: Prototype Crab Sampling Device

The crab sampling device has been designed to allow marine researchers to collect juvenile crabs measuring less than 50mm across its back, from a known area, under repeatable conditions and to disturb the seabed so that they cannot burrow or hide. All this was to be accomplished without having to dive for them. From an anchored vessel sitting at the surface of the water, the sampling device can be lowered into the water using mechanical hoists. The sampling hood defines a fixed sample area, sitting firmly at the bottom of the ocean. While the jets inside the sampling hood stir the sample area, suspended objects (hopefully juvenile crabs) will be transported via hoses to the water

surface, into a catchment cage. From there, the numbers and size of the crabs can be recorded and they can be returned, unharmed to the seabed.

5.1 SYSTEM ANALYSIS

The duty of the jet pump for this application is primarily for transporting the crabs from the sea floor to the water surface. It will not have to do any work in terms of lifting the crabs above the water surface, so that the jet pump can be throttled to operate at a lower pressure. A more gentle form of pumping then results. Most of the load on the jet pump will therefore, be due to frictional and hydraulic factors only. This makes the system curve rather simple. Applying Bernoulli's theorem between a & s:

$$\frac{P_a}{\rho g} + \frac{V_a^2}{2g} - Z_a = H_s + H_{ls} \quad [5.1]$$

Where H_{ls} is the frictional head losses encountered between a & s. Next, noting that $P_a/\rho g = -Z_a$ and $V_a = 0$:

$$H_s = -H_{ls} \quad [5.2]$$

Similarly, between d & c:

$$H_d = \frac{P_c}{\rho g} + \frac{V_c^2}{2g} + Z_c + H_{lc} \quad [5.3]$$

Where H_{lc} is the head losses between d & c. Noting that P_c is at the free surface, $P_c = 0$, $V_c = 0$ and $Z_c = \text{datum} = 0$:

$$H_d = -H_{lc} \quad [5.4]$$

Substituting [5.2], [5.4] and expanding for H_m in equation [2.2]:

$$N = \frac{H_{lc} + H_s}{\frac{V_m^2}{2g} + \frac{P_m}{\rho g} - Z_m + H_{ls}} \quad [5.5]$$

Equation [5.5] can be regarded as the general system curve equation for underwater, zero-lift conditions. Additional analysis is then required to transform the relationship in

terms of Q_m and M , so that it can be combined with equation [2.18]. The operation point can then be found either graphically or analytically, similar to that for the fish pump application.

5.2 EXPERIMENTS & RESULTS

During the development of the sampling hood, several different designs were tested for effectiveness. Both laboratory and field tests were conducted until a final design yielding reasonable results was found. Only some of the results from the final sampling hood design are presented here. Figure 27 shows some of the final sampling hood design details. Note the existence of an intake ventilation slot on the top perimeter of the sampling hood. This slot is beneficial to the overall smoothness of the flow, induced by the 60 jets. Reduced randomness of the flow inside the hood was observed when the slot was incorporated into the design.

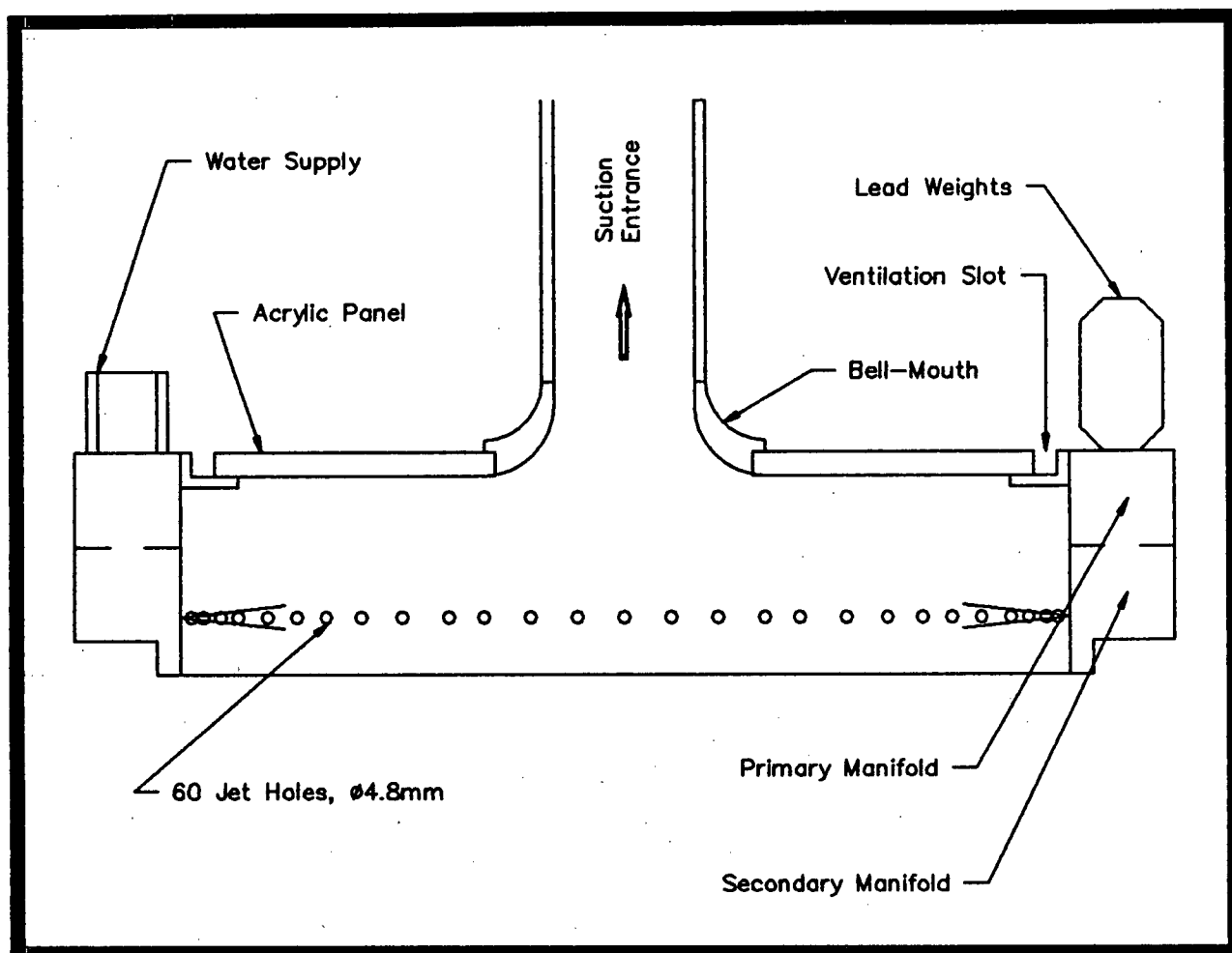


Fig. 27: Sampling Hood Details

Optimizing the Sampling Hood Jets

In an effort to determine the best jet hole diameter for the sampling hood, experiments were carried-out using sea shells as models for crabs. The complete sampling system was set-up in the laboratory. A tank with a clear acrylic side permitted visual observation of the effectiveness of the sampling hood jets. The number of jet holes were varied until a suitable design at 60 holes was found. For designs less than 60 holes, the flow inside the sampling hood was too erratic. More than 60 holes required diameters which were so small, that

clogging became a problem. Six different sampling hood jet diameters between 3.2mm and 6.4mm were tried.

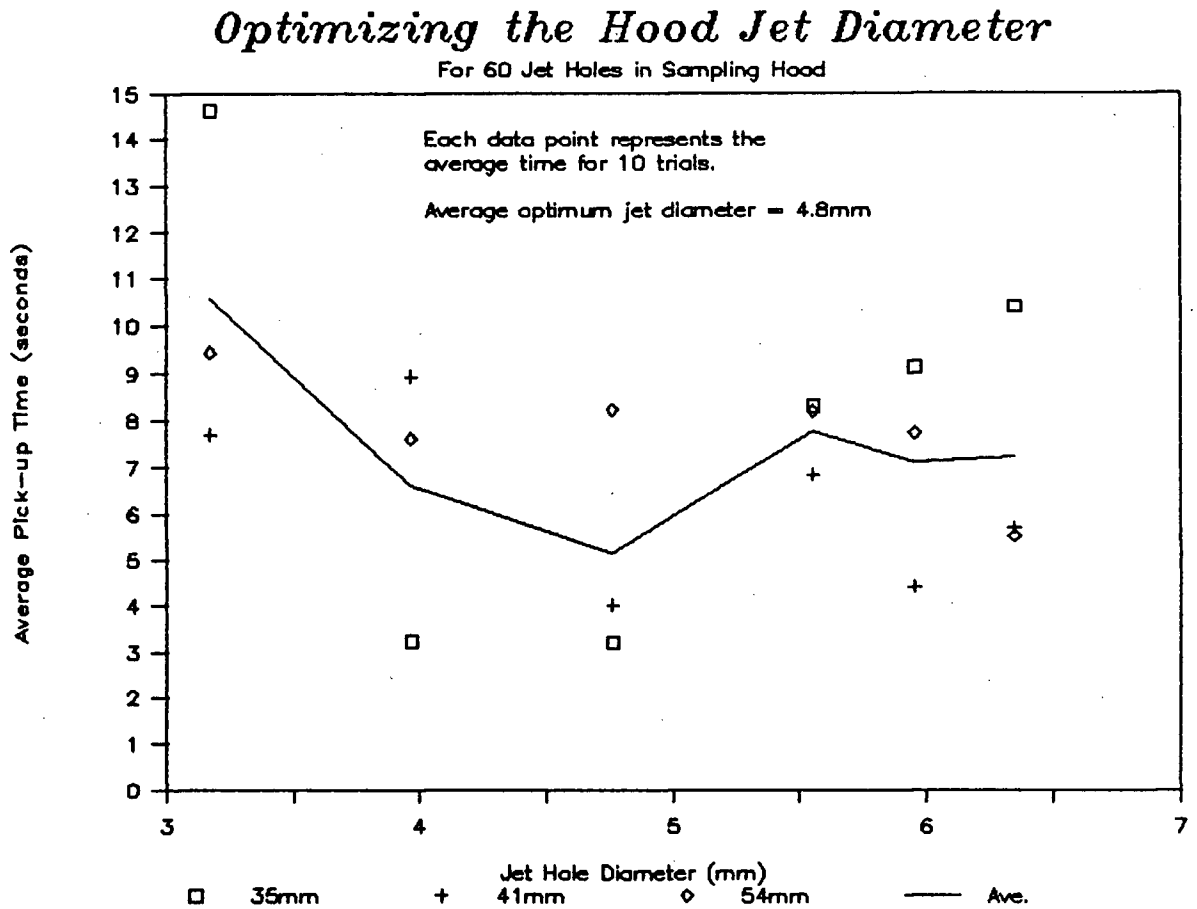


Fig. 28: Minimizing Pick-up Time

With the complete system operating, 35mm, 41mm & 54mm shells were individually placed under the sampling hood. Each shell was timed until the sampling hood jets were able to pick-up and place the shell into the transport hose. For each shell size, 10 trials were averaged for one data point on the graph. The results are shown in figure 28.

A jet hole diameter of 4.8mm gave the best averaged result, and was subsequently used in the final design.

Field Tests

In actual field tests, the crab sampling system did not work as reliably as wanted. The main difficulty was in gathering the crabs near the vicinity of the suction entrance. Once the crabs were inside the suction hose, however, no problems were encountered. The jets in the sampling hood were sometimes too powerful, shooting the crabs right across the suction entrance. Yet, at times, the jets were too weak, failing to pry clinging crabs from rocks and kelp. The crab sampling system has good potential for success, however, it needs a better method of herding the crabs into the suction hose.

6. APPLICATION AS A BOW THRUSTER

Bow thrusters are used for lateral maneuvering on large ships. Two categories of thrusters currently exist on the market: 1) the simple propeller units and 2) the water jet units. Although the propeller units are the most commonly used, they do have their drawbacks. They are prone to propeller damage, reduced efficiency in presence of cross-currents, ineffective in rough seas where propeller may rise out of the water. Also, propeller units require an uninterrupted flow of water for maximum efficiency.

Shortcomings in the propeller design eventually led to jet propulsion systems. The advantages of this system are many: faster response time, maintains effectiveness in cross-currents and in rough seas, and is less likely to be damaged due to debris. Unlike propeller units, jet systems usually have water intakes which are well below the water surface. This ensures a continuous source of supply.

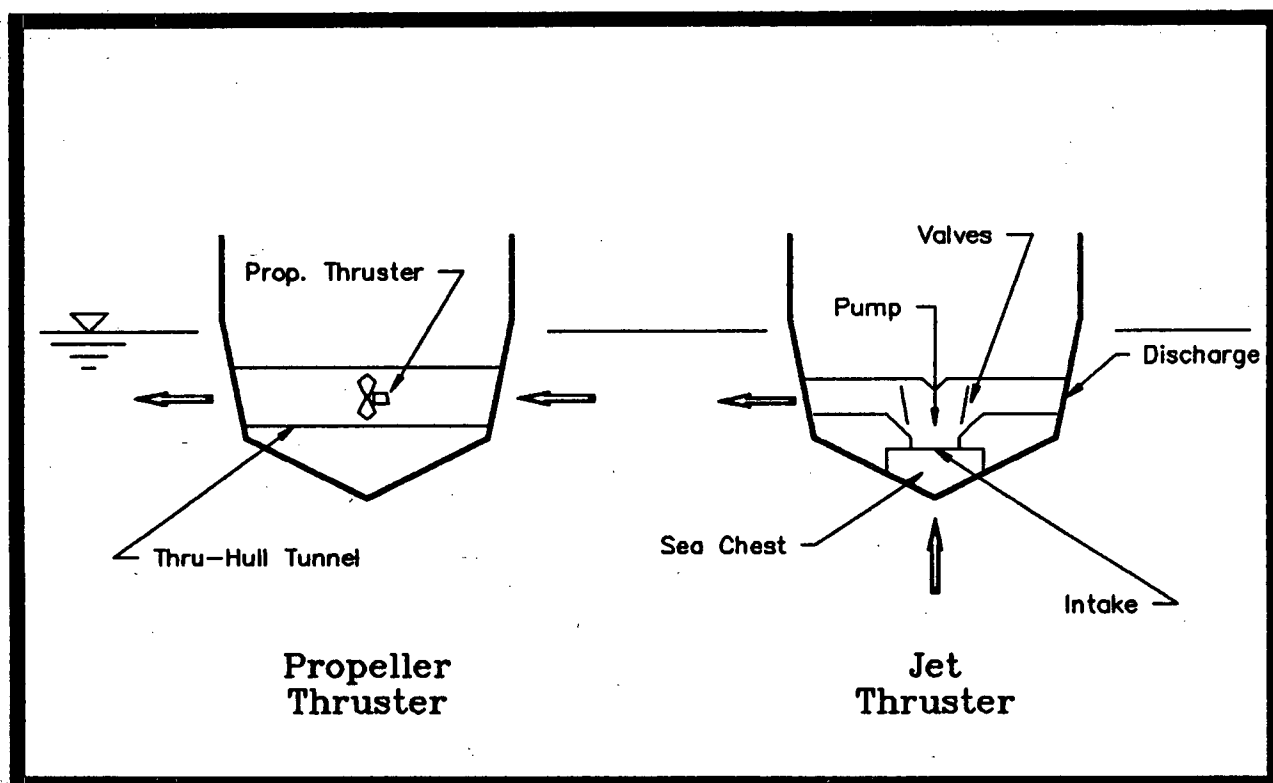


Fig. 29: Propeller & Jet Thrusters.

The governing criteria for good thruster designs are based around maximizing the developed momentum. This will yield maximum forces to be exerted on the surrounding water, which provides the required propulsion for ship movement. Thus, for this application, the jet pump will be designed for maximum momentum.

Also of concern is the specific thrust of the thruster. This is a measure of performance for various thrusters, and is defined as the quotient of output force per unit power. For simple propeller thrusters, the claimed specific thrusts are near 136N/kW (24lbs/HP). For jet thrusters this figure is near 119N/kW (21lbs/HP). These are the standards to which the jet pump thruster can be compared.

The proposed jet pump application is shown in figure 30.

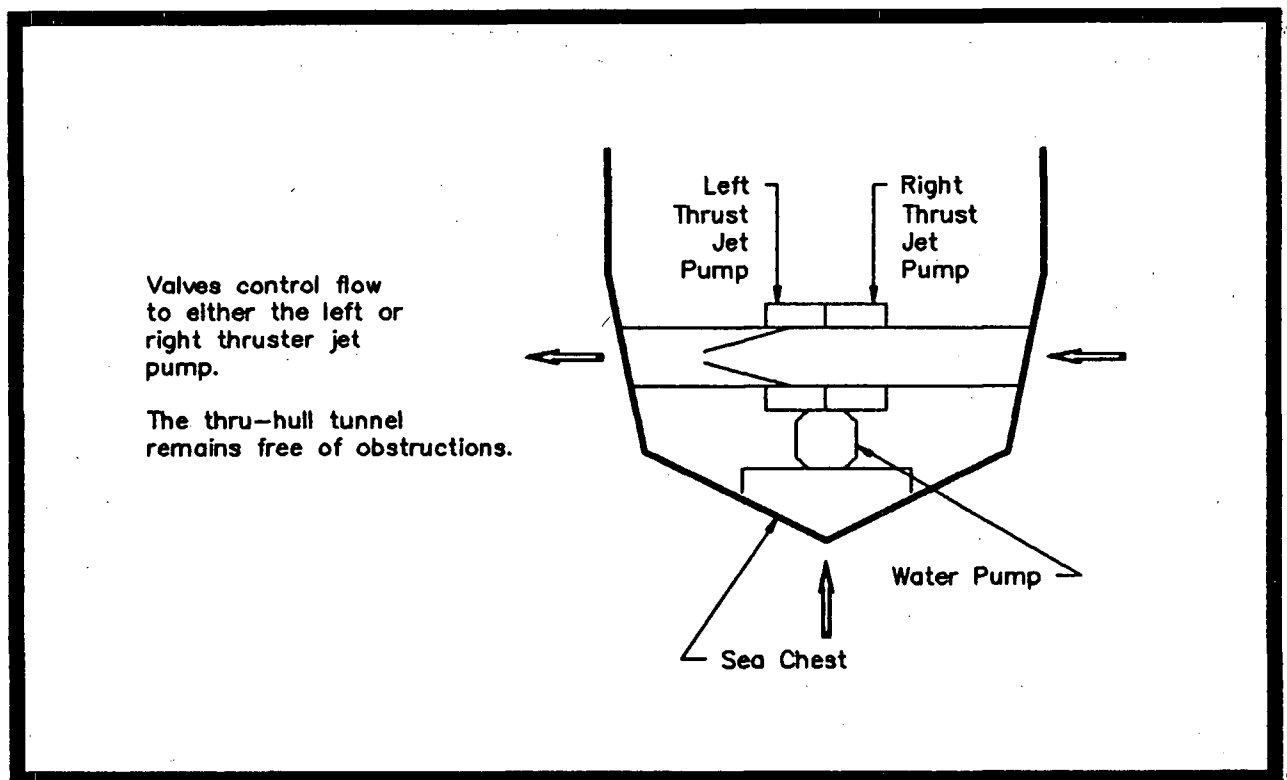


Fig. 30: Jet Pump Thruster

6.1 SYSTEM ANALYSIS

Following in the same fashion as the fish pump and crab sampling device, the jet pump can again be analyzed for application in a thruster setting. The simple analysis has been omitted, but the resulting system curve equation is given below:

$$N = \frac{(1+K_{lc})(M+1)^2 + (K_s-1)M^2}{\frac{(1+K_2)}{R^2} - M^2} \quad [6.1]$$

where

K_{lc} = (sum of the discharge K-factors),

K_s = (sum of the suction K-factors).

Notice that this system curve is completely dimensionless, and therefore, it can be plotted on the N-M graph, along with the pump curve [2.18]. The intersection of [6.1] and [2.18] will define the operating N & M values for the system.

A force-momentum analysis yields the following relationships for thrust and power:

$$\text{Thrust} = F_x = \frac{P}{A} [(1+0.5K_3)(Q_m+Q_s)^2 - Q_s^2] \quad [6.2]$$

$$\text{Power} = Q_m \rho g H_m \quad [6.3]$$

where K_3 = shear factor for the thruster tunnel. This value was estimated from tables of friction factors and is taken to be 0.2.

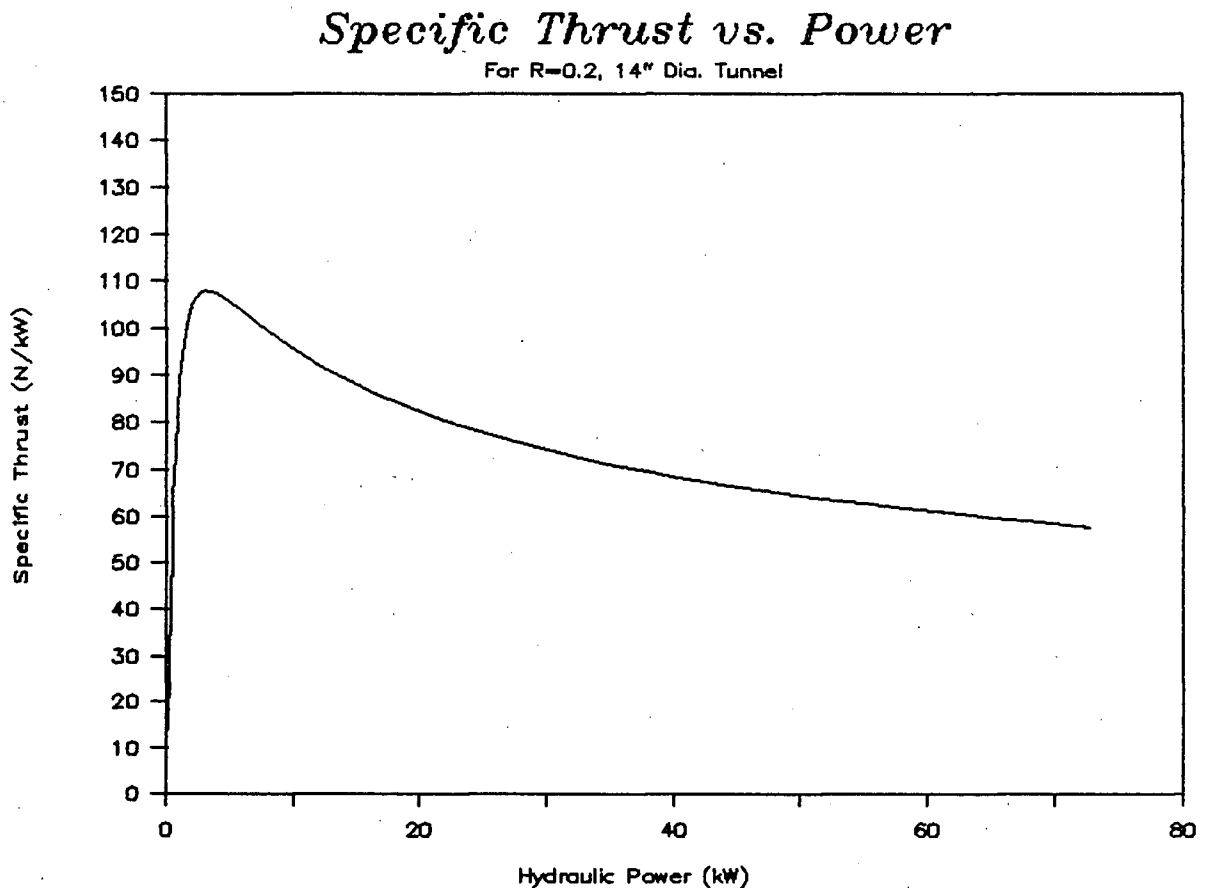


Fig. 31: Specific Thrust

The specific thrust graph of figure 31 shows the variation as the input power is increased. Assuming a 356mm (14") diameter tunnel, the specific thrust quickly reaches its maximum of 109N/kW (19lbs/HP) at 2kW, then it reduces to only 51N/kW (9lbs/HP) at 75kW. Since the normal operating range for thrusters is beyond 40kW, the jet pump thruster will not normally be operating at its maximum specific thrust. Therefore, the specific thrust at normal operation will only be about 51N/kW. This is far below the 136N/kW & 119N/kW standards set by the current propeller and simple jet thrusters.

The jet pump thruster fails to achieve the level of performance of existing designs, however, it may have specialized applications when performance is not the major criterion.

Installations in ice-breakers, may be one such application. The determining factor for these vessels is the operability under adverse conditions, including ice debris. Otherwise, the jet pump is not a strong contender for thruster applications. Further studies in this application may not produce any appreciable increase in performance.

7. DISCUSSION

Laboratory Model

Simple one-dimensional theory for the tested jet rings did not correlate closely to experimental results (refer to figure 7). Possible reasons for this may be due to reduced jet momentum for wide spraying jets and deviations in the jet geometry, such as jet hole diameter and spray angle. Small deviations between the assumed geometry and the actual geometry are inevitable, but limits on improvements for this correlation is quickly reached. The governing one-dimensional theory, however, has considerable room for improvement. Currently, the assumed jet momentum is $\rho Q_m V_j$, and according to Westfall (14), this is an acceptable valuation for narrow spray patterns. But for jets which have wide spray patterns, evidence presented here indicate that this estimation does not hold. A suggested modification is, to add a spray width factor, K_w , to the momentum. The jet momentum would then be $K_w \rho Q_m V_j$, where K_w is less than unity. After further studies, empirically derived relationships between K_w and the widening of the jet spray can be derived. Then, jet pump experiments can be remodelled to determine the validity of the modified one-dimensional theory.

The importance of relative jet lengths in jet pumps has been noted. As the relative jet length, R.L., decreases, the jet spray pattern widens. With a decrease in R.L., the suction performance increases, but the lifting head performance decreases. Both of these characteristics can be explained by the following suggestions.

For suction performance, the criterion is the amount of jet shear area. This is the surface area of the jets, where the actual development of shear occurs. Any other portion of the jet (the central core, for example), is not used for the development of shear stress. Wide spray patterns would then have larger jet shear area than narrow spray patterns. This accounts for the increase in suction performance as the width of the spray pattern increases.

Also, it was observed that maximum vacuums were not developed until the volume in the suction inlet was filled with water. This supports the jet shear concept, because shear stress between the jets and water should be greater than between the jets and air. The developed shear when the suction inlet is full of air, will be small compared to when the suction inlet is full of water. Therefore, the development of maximum vacuum will not occur until water fills the suction inlet.

For lifting performance, the criterion is the amount of injected momentum in the desired direction of flow. This proposes that the jets be narrow and directed axially down the mixing chamber. With narrow jets, the momentum would be maximized, with the proposed spray width factor, $K_w = 1$. Wider jets would decrease the momentum a corresponding amount, according to the value of $K_w < 1$.

The jet angles also affect the momentum by a factor given by $\cos\Theta$. For jets oriented axially, the momentum will not be reduced by this factor. However, this geometry is not possible for the current peripheral jet pump design. New geometries would be needed for the case where $\cos\Theta = 1$.

In general, the momentum available from the jets which contribute in the desired direction is equal to: $K_w \rho Q_m V_j \cos\Theta$. This term can replace the corresponding term as given in equation [2.7].

When pumping solids, maximum forces on the solid can be induced with the jet pump out of the water, in the unsubmerged condition. The solids must be tossed into the water jets where they can be subsequently carried away in swirling water and air. This causes large stresses on the solid, therefore, it is not the recommended mode of operation for handling fragile materials. With the jet pump submerged, a much smaller force is applied on the solid. If the solid is then introduced to the system, the surrounding water acts as a buffer to dissipate the force of the jets. The overall effect is reduced contact force on the solid. In the

example illustrated earlier, it was found that 64.4N of force would be applied to a solid if the jet pump was unsubmerged, and 25.6N if the jet pump was submerged.

It was observed that, in the 95% submerged state, the jet pump's ability to handle solids was superior to that of the fully submerged state. The formation of vortices at the suction inlet, helped to entrain floating solids into the jet pump. Surface tension effects were also thought to provide much of the pulling action of the floating solids. As the jet pump drew-in the surface layer of the water, it brought with it, the solids which were held by the surface tension. This ability to simultaneously pump solids, liquids and gases is unique to jet pumps.

As a Fish Pump

Although some difficulties in fish damage were encountered, good potential lies in the use of the jet pump as a fish transport system. Additional research on improving the jet design to reduce the scale-loss and other fish damage will be required. More extensive laboratory testing of the jet profiles and configurations should yield a better solution to this problem. Some suggested tests are:

- Vary the number of water jets (16, 18, 20 or 24 jet holes). This increases the jet shear area, which was found to have positive increases in the jet pump's vacuum performance. This will be an important factor to determine, so that better solids entrainment can be established.
- Vary the number of jet perimeter locations. Rings #1 - #3.1 all had 16 jets exiting at one perimeter location. Only the Hillis had jets at two locations (8+8 jets, see figure 6). Other designs with two and three perimeter locations should be experimented with. For example, try 16+16 jets. This affects the distribution of the momentum over a larger volume, which decreases the momentum injected by each individual jet. The jet

shear area will also be increased. The results may indicate a reduction in fish damage, and a net increase in the suction performance.

- Operating under partially submerged conditions at inlet seemed to improve the solids handling capability. Therefore, it may be useful to investigate the effects of deliberate air injection. Although the prototype fish pumps were made with air-injection capability, thorough testing of its effects were not conducted.

As a Crab Sampler

The jet pump performed well under this application. Unlike the fish pump, it was not required to lift the product high out of the water, therefore, the only major system load on the jet pump was friction in the hoses. All of the juvenile crabs which passed through the jet pump survived, despite the stress of the jets. The hard outer shell protected these crustaceans from injury.

The basic design of the sampling hood is satisfactory, especially with the incorporation of the ventilation slot. But the design still needs further work to achieve a smoother sampling of the crabs. At present, the crabs are disturbed randomly, and collected as they are passed across the suction inlet. Given sufficiently long sampling times, eventually all of the crabs will be pushed across the suction inlet, and taken by the effects of jet pump.

It must be realized that entrainment of sediment and crabs is bound to be a turbulent process, by its very nature, and this makes direct observation of the crab removal difficult. But with additional funding to research the sampling hood, a fully functional crab sampling system can be developed. It will help crustacean researchers collect specimens from the ocean floor, without having to dive to get them.

As a Bow Thruster

Unfortunately, the jet pump thruster fails to be competitive with existing maneuvering systems. Propeller thrusters claim specific thrusts up to 136N/kW (24lbs/HP), jet thrusters claim 119N/kW (21lbs/HP), while jet pump thrusters can only reach 51N/kW (9lbs/HP). For an industry that is power-conscious, the kind of performance required from thrusters, will still remain dominated by propeller and jet thrusters. Ice-breaker installations, where functionality and not efficiency is the major concern, is a potential application for the jet pump thruster. Ice and other floating debris, which may damage propeller type thrusters, will not be a concern for the jet pump. It will easily produce thrust regardless of the debris in the water. Only then will the jet pump thruster show to be a worthwhile contender.

8. CONCLUSIONS

Improvements in the one-dimensional theory are needed to better correlate with experiment for jets having wide spray patterns. The existing theory fails to accurately model the momentum injected by the jets. A correction factor, K_w , for the jet momentum, $\rho Q_m V_j$, should now be tried in both theory and experiment. Additional studies in determining appropriate values for K_w need to be conducted.

For suction performance, larger jet shear areas will yield better results. Tests showed that wide spray patterns, which have larger jet shear area than their narrow equivalents, are better equipped for this purpose. It should be noted that vacuums do not fully develop until the suction inlet is full of water, such that the jets are spraying into water instead of air. Additional studies where jet geometries are changed, should be investigated for its effect on suction performance.

For maximum lifting performance, the best jet configuration is when the injected momentum is maximized. This implies narrow, stream-line jets, which are aimed directly in the direction of flow. For the peripheral jet pump geometry in this study, it is not possible to aim the jets in the direction of flow, however, this point should be taken into consideration for future designs.

The solids-pulling ability was found to be optimum when the jet pump was tilted on its side, with the front inlet about 95% submerged in the water. The 95% submergence creates a partial blockage, which has been found to be beneficial to the suction performance. While 95% of the front inlet is creating a vacuum, the other 5% is producing air-&-solids-entraining vortices. With the aid of surface tension, the vortices swirl any nearby floating solids into the inlet.

Generally, the jet pump performance can be improved with the distribution of the jet momentum. Geometrically, this requires that the number of jet holes be increased. But to

maintain constant area ratio, R , the individual jet diameters must be reduced accordingly. By doing this, three of the desired characteristics found from this study is satisfied.

Firstly, the jet shear area will be increased, therefore, an increase in the suction performance should result.

Secondly, because the relative jet length of each individual jet increases, the loss in momentum due to spreading of the jets does not occur. The proposed width correction factor, K_w , can still remain at unity. This should result in better lift performance.

Finally, the major effect of the distribution is the reduction of momentum per jet. This should prove to have a much more gentle action on the solids passing through the jet pump. This will be especially beneficial for pumping delicate solids such as live salmon.

As a further refinement of the distribution of momentum, jets can be drilled at an oblique angle, such that a rotation is induced in the mixing chamber. This should increase the available jet shear area, since the jets will now travel a greater distance before interference from adjacent jets. The effects of oblique jet angles may be small, but this can not be known with certainty until further studies are undertaken.

9. REFERENCES

For introductory reading material, two references are suggested: a) Stratton's article "Liquid Jet Ejectors..." and b) Jumpeter's "Jet Pumps." For jet pump theory based on one-dimensional flow, see papers written by, Cunningham, Henzler, Jumpeter, Kentfield et al and Westfall. For jet pump theory based on two-dimensional flow, see papers written by, Charlesworth et al, Hill and Hongji et al. For jet pump theory based on empirical formulas, see Xianghan.

- (1) Birkhoff, Garrett and Zarantonello, E.H. Jets, Wakes, and Cavities, (Academic Press Inc. 1957).
- (2) Charlesworth, A., Croft, David R. and Lilley, David G., "Prediction of Jet Pump Performance Using a Finite-Difference Primitive Variable Technique," Paper presented at 3rd Nat. Comp. Physics Conf., Glasgow, UK, (August 1975), Transcripta Books, London and Hemisphere Pub. Corp., Washington, D.C., (in press 1976).
- (3) Cunningham, R.G., "Liquid Jet Pump Modelling: Effects of Axial Dimensions on Theory-Experiment Agreement," Proc. 2nd. Symp. Jet Pump & Ejectors and Gas Lift Techniques, (BHRA Fluid Eng. 1975), pp. F1:1-15.
- (4) Henzler, Hans-Jurgen, "Design of Ejectors for Single-phase Material Systems," Ger. Chem. Eng., (Vol.6, 1983), pp. 292-300.
- (5) Herbich, John B. Ph.D., P.Eng. "Jet Pumps in Dredging," Coastal and Deep Ocean Dredging, (Gulf Publishing Company, 1975), pp. 343-375. VPL 627.73 H53C
- (6) Hill, B.J., Journal of Hydraulic Division, ASCE, (Vol.99, 1973).
- (7) Hongji, Lu and Xiangjin, Zeng, "Studies on Liquid Jet Pump," Scientia Sinica, (Vol.24, April 1981), pp. 581-593.
- (8) Jumpeter, Alex M. "Jet Pumps," Pump Handbook, (Edited by Igor J. Karassik, 1976), pp. 4:1-25.
- (9) Kentfield, J.A.C. Ph.D. and Barnes, R.W. "The Prediction of the Optimum Performance of Ejectors," Proc Instn Mech Engrs, (Vol. 186 54/1972), pp. 671-680. TJ1 I5 Vol.186

-
- (10) "Fishtails, Water Jets and Wheels," Marine Engineer's Review, (Vol.87, No.2, 1982), pp. 91-104.
- (11) Rajaratnam, N. "Turbulent Jets," Developments in Water Science, (No. 5, 1976).
- (12) Schetz, Joseph A. "Injection and Mixing in Turbulent Flow," Progress in Astronautics and Aeronautics, American Institute of Aeronautics and Astronautics, (No. 68, 1980). TA 357 S33.
- (13) Stratton, Harry, "Liquid Jet Eductors- The Pumps With No Moving Parts," Plant Engineering, (April 29, 1976), pp. 215-218.
- (14) Westfall, Alan Patrick, "Peripheral Jet Pump Theory and Experiment," Master's Thesis, The University of British Columbia, 1983.
- (15) Xianghan, Hu, "Research of the Design Theory for Liquid State Jet Pumps," Scientia Sinica (Series A), (Vol.26, February 1983), pp. 214-224.